

UNCLASSIFIED

AD **408 551**

DEFENSE DOCUMENTATION CENTER

FOR

SCIENTIFIC AND TECHNICAL INFORMATION

CAMERON STATION, ALEXANDRIA, VIRGINIA



UNCLASSIFIED

NOTICE: When government or other drawings, specifications or other data are used for any purpose other than in connection with a definitely related government procurement operation, the U. S. Government thereby incurs no responsibility, nor any obligation whatsoever; and the fact that the Government may have formulated, furnished, or in any way supplied the said drawings, specifications, or other data is not to be regarded by implication or otherwise as in any manner licensing the holder or any other person or corporation, or conveying any rights or permission to manufacture, use or sell any patented invention that may in any way be related thereto.

408 551

63-4-2

408551

MEMORANDUM

RM-9156-PR

JUNE 1963

CATALOGED BY DDC

AS AD NO. 408551

OCEAN-CURRENT MODELS USING
POTENTIAL VORTICITY

Robert R. Blandford

RECEIVED
JUL 16 1963
TSEA A

PREPARED FOR:

UNITED STATES AIR FORCE PROJECT RAND

The RAND Corporation

SANTA MONICA • CALIFORNIA

MEMORANDUM

RM-3156-PR

JUNE 1963

**OCEAN-CURRENT MODELS USING
POTENTIAL VORTICITY**

Robert R. Blandford

This research is sponsored by the United States Air Force under Project RAND—contract No. AF 49(638)-700 monitored by the Directorate of Development Planning, Deputy Chief of Staff, Research and Development, Hq USAF. Views or conclusions contained in this Memorandum should not be interpreted as representing the official opinion or policy of the United States Air Force.

The **RAND** *Corporation*

1700 MAIN ST. • SANTA MONICA • CALIFORNIA

PREFACE

The increasing interest in water-based systems, such as oceanic basing of missile and space-tracking systems, stimulates original contributions of basic research pertaining to a relatively unknown and relatively little-understood operational environment. This Memorandum develops theoretical models and compares them with observed data for the Gulf Stream and the Cromwell Current.

SUMMARY

Two-layer and continuous models of the Gulf Stream and one-layer and continuous models of the Cromwell Current, respectively, are developed from theoretical considerations. Numerical results obtained from computer solutions of these models are compared with observed data and are found to show reasonably good agreement. The limitations of the modeling are set forth.

CONTENTS

PREFACE	iii
SUMMARY	v
LIST OF SYMBOLS	ix
Section	
I. INTRODUCTION	1
Gulf Stream	1
Cromwell Current	2
II. THE GULF STREAM--THE EXPERIMENTAL DATA	4
The One-Layer Model	4
Two-Layer Models	15
Rotation of Co-ordinate System to Stream Axes	24
The Continuous Case	26
III. CROMWELL CURRENT	47
Theory of the Cromwell Current	47
One-Layer Model	53
IV. CONCLUDING REMARKS	68
Appendix	
A. THE CONTINUOUS-MODEL CORE	69
B. DERIVATION OF POTENTIAL-VORTICITY EQUATION	72
REFERENCES	79

LIST OF SYMBOLS

- A_H = coefficient of horizontal eddy velocity
 A_V = coefficient of vertical eddy velocity
 a, a_1, a_2, a_i = coefficients
 b, b_1, b_2, b_i = coefficients
 b_r = known value on the boundary
 c = coefficient
 D, D_1, D_2 = thickness of a stream layer
 D_∞ = thickness of the stream layer at infinity
 D_1^0, D_2^0 = thickness of the stream layer 1, 2 at infinity
 f = coriolis parameter
 g = acceleration of gravity
 $g' = g(\rho_2 - \rho_1)/\rho_2$
 h = height of the free surface
 h_1, h_2 = height of the free surface of layer 1, 2
 \hat{h} = dimensionless variable h/h_0
 $K = \text{constant} = (\rho_b - \rho_s)/2\rho_b$
 \underline{K} = force vector, due to friction, etc.
 L = length of path
 L = as superscript, indicates stream left of axis
 M = as superscript, indicates stream between stream L and stream R
 n = ratio of the thickness of a layer at the equator to the thickness at y_0
 o = as subscript or superscript, indicates at infinity
 p = pressure
 P_1, P_2 = pressure in layer 1, 2
 p = as subscript, refers to "warm core" peak
 $q = 7 \times \underline{V}$
 R = radius of the earth
 R = as superscript, indicates stream right of axis
 r = vertical co-ordinate = $(\rho_b - \rho)/(\rho_b - \rho_s)$
 $r(s)$ = vertical co-ordinate defining the surface
 $r(b)$ = vertical co-ordinate defining the bottom boundary

- $\underline{S} = \underline{\gamma} \alpha \times \underline{\gamma} p$
u = velocity component in x direction
 u_j = unknown value in the interior
 \underline{u}_x = velocity with reference to the earth
 \underline{u}_a = velocity with respect to the inertial system
v = velocity component in y direction
 v_1, v_2 = velocity components in y direction of layers 1, 2
v = dimensionless variable = $v/\sqrt{2Kgh_o}$
x = horizontal co-ordinate
 x_p = co-ordinate of the "warm core" peak
 \hat{x} = dimensionless variable = $x/\sqrt{2Kgh_o/f^2}$
y = horizontal co-ordinate
 $y_b = (2Kgh_o/B^2)^{1/4}$
 y_{ch} = critical fall-off distance for Δ
 \hat{y} = dimensionless variable = $y\gamma^{1/4}$
 $Z(r)$ = function giving the z co-ordinate of water with density co-ordinate r
 $Z_o(r)$ = function giving the z co-ordinate infinitely far to the right of water with density co-ordinate r
 $Z'_o = \frac{\partial Z_o(r)}{\partial r}$
 $Z''_o = \frac{\partial^2 Z_o(r)}{\partial r^2}$
 Z'_p = peak value of Z'
 $\hat{Z}_o = \text{dimensionless variable} = Z_o/h_o$
z = vertical co-ordinate
 $z(r)$ = vertical co-ordinate, function of r
 $z(s) = h$

- α = reciprocal of density (Appendix B)
 α = numerical coefficient
 $\beta = D_1^o/D_2^o$ (two-layer model of Gulf Stream; pp. 17-19)
 $\beta = \frac{\partial}{\partial \theta}$ (derivative of a coriolis parameter)

$\gamma = \Delta\rho_1/\Delta\rho_2$ (two-layer model of Gulf Stream; p. 18)

$\gamma = \beta^2/g'h_0$ (one-layer model of Cromwell Current; p. 53)

$\Delta = z(r) = Z_0(r)$

$\hat{\Delta} = \Delta/h_0$

$\zeta = \frac{\partial v}{\partial x} - \frac{\partial u}{\partial y}$

$\eta = [\text{curl } v + \nabla \times (\omega \times r)]$

$\theta = \text{latitude}$

$\lambda = \sqrt{g'D_0/f^2}$

$\lambda = \text{radius of deformation (Appendix B)}$

$\xi = \hat{y}^2/z$

$\rho = \text{density}$

$\rho_1, \rho_2, \rho_3 = \text{density of layer 1, 2, 3}$

$\rho_s = \text{density at the surface}$

$\rho_b = \text{density at the bottom of region of interest}$

$\rho(\) = \text{density function of}$

$\sigma_t = \text{density parameter} = 1000(\rho - 1)$

$\chi = q \cdot \alpha \cdot 7 \psi$

$\psi = \text{stream function}$

$\Omega = \text{angular velocity of the earth}$

$\underline{\omega} = \text{angular velocity vector of the earth}$

I. INTRODUCTION

This analysis applies the concept of potential vorticity* to two ocean currents--the Gulf Stream and the Cromwell Current. First, the experimental data for the Gulf Stream are reviewed. Then Stommel's⁽¹⁾ simple one-layer model of the Gulf Stream is discussed, and the assumptions necessary to the theory are explicitly stated. This model contains no variable parameter. Appendix A contains important modifications that should be scanned before a careful reading of the body of the Memorandum.

GULF STREAM

A two-layer theory is developed along the lines of Stommel which gives, semiquantitatively, the features of an inertial countercurrent and the recession of the axis of maximum velocity under the Gulf Stream. Note that the theory is only a consistency argument and does not consider cause and effect.

Next, it is shown that writing the equations of motion as if the stream headed due north at the point where the theory is to be applied gives almost no error.

The continuous theory is developed. The density is used as a vertical co-ordinate, and in this co-ordinate system the assumption of a level of no motion leads to a Laplace-type equation to be solved in a specified region with given boundary values. It enables us to calculate the density and velocity of a cross section of the Gulf Stream

* Defined as vorticity of the water divided by the local gradient of any conserved field. In this study, the density is the only such field used.

if we know only the density structure on the boundaries of the cross section. First, a simple analytical model is solved for a linear density gradient above a region of constant density. Next, a solution that agrees well with observation is obtained by computer, using observed data as input data on the boundaries.

Finally, a discussion of the possible effects of friction on the accuracy of the solution is given in Appendix B. To discuss these effects, it is necessary to derive the conservation of potential vorticity in general form. The results show that if the Navier-Stokes expression is used for viscous stresses, then for $A_H \leq 10^5 \text{ cm}^2/\text{sec}^*$ and $A_V \leq 10 \text{ cm}^2/\text{sec}^{**}$ we may get negligible effects. This completes the investigation of the Gulf Stream.

CROMWELL CURRENT

The hypothesis that the water of the Cromwell Current sinks at 3° north or south latitude, moves to the equator, rises to the surface and moves back to the same latitude is shown to be improbable because of salinity data and because of certain dynamic considerations. It is assumed that this water comes from a source extending across the equator and therefore that its potential vorticity is highly variable. Simple models are used to show the reasonableness of this view. The assumption is made that the potential vorticity of a parcel of water is proportional to its distance from the equator. This is because the source of water found at some distance from the equator is likely to be farther from the equator than a parcel found on the equator.

* A_H = Coefficient of horizontal eddy viscosity.

** A_V = Coefficient of vertical eddy viscosity.

Under this assumption, the continuous case is developed for the Cromwell Current, and a computer solution gives the three layers of this case, one above the other, semiquantitatively, using as input data the density structure at the equator, on the surface and at 4° latitude. There is, unfortunately, a variable parameter in the theory-- which can probably be measured--to represent the distance from the equator of the source of a parcel of water.

Adjustment of this parameter for best fit to the data gives a narrow source region of width about 4° of latitude. The results are rather insensitive to the value of the parameter. Finally, in Appendix B, the limitations of this theory of the Cromwell Current due to friction and vertical velocities are considered. Here, in contrast to the Gulf Stream, values of $A_v = 5 \text{ cm}^2/\text{sec}$ might seriously invalidate the theory.

II. THE GULF STREAM--THE EXPERIMENTAL DATA

A cross section of the Gulf Stream reveals that lines of constant temperature and salinity rise as one follows them from east to west. This fact is illustrated in the cross sections taken by Iselin,⁽²⁾ shown in Figs. 1 and 2. In the temperature section by Iselin we see a typical feature of the Gulf Stream, the "warm core" that in this case is bounded by the 20°C isotherm near Station 1227. Usually, associated with this warm core is a countercurrent which is seen, for example, in the velocity cross section computed by Neumann⁽³⁾ and shown in Fig. 3. Neumann's section shows that the point of maximum velocity for a given depth recedes eastward under the Gulf Stream. It is also notable that the maximum velocity of the countercurrent recedes westward. The order of magnitude of both these slopes is 1/50. We also see that both the 10°C and 4°C isotherm fall a fraction $(1 - e^{-1})$ of the vertical distance between their western and eastern elevations in a west-east distance of about 90 km.

Figure 4, by Iselin, shows the depth of the 10°C isotherm in the western North Atlantic. These lines to a large extent parallel the actual transport lines of the water feeding into the Gulf Stream as drawn by Iselin. A cross section of Iselin's along the 42° meridian of longitude is shown in Fig. 5.

THE ONE-LAYER MODEL

Review of Previous Work

To illustrate the spirit in which this analysis will be developed, let us review briefly a one-layer model of the Gulf Stream by Stommel.⁽¹⁾

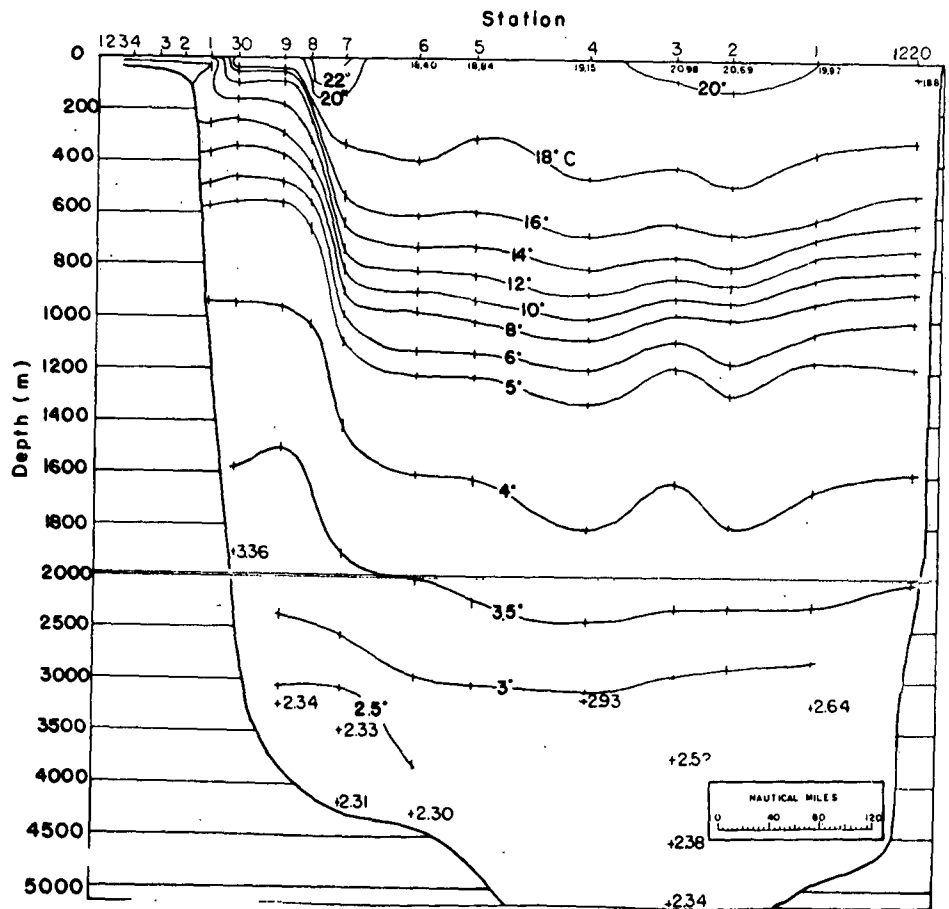


Fig. 1 -- Temperature section across the Gulf Stream--
Chesapeake Bay to Bermuda (2)

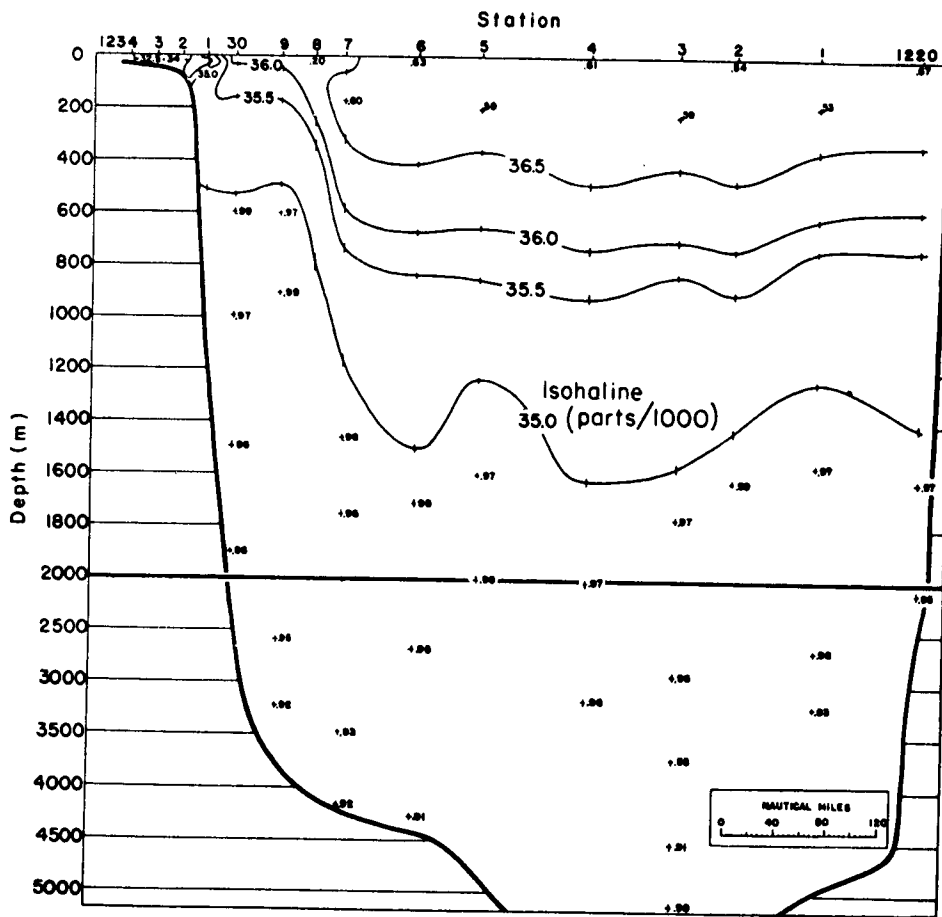


Fig. 2 -- Salinity section across the Gulf Stream--
Chesapeake Bay to Bermuda (2)

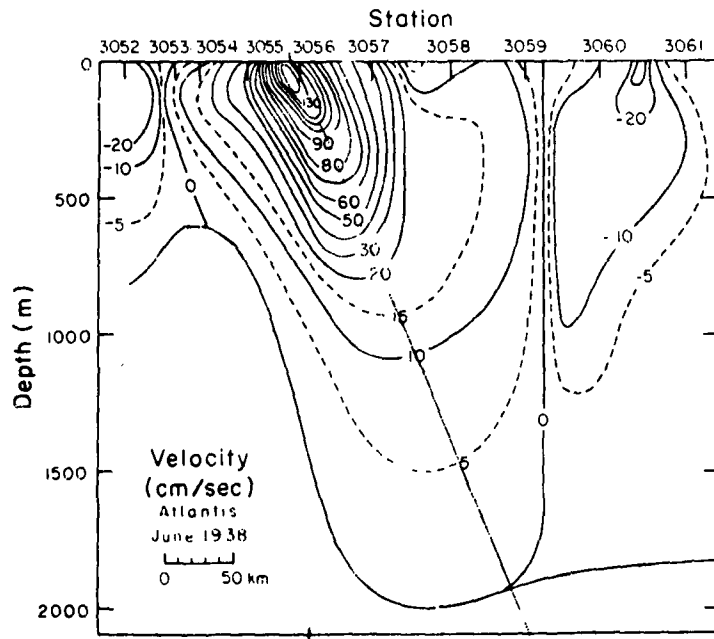


Fig. 3 -- Typical velocity cross section of the Gulf Stream from Montauk Point to Bermuda (3)

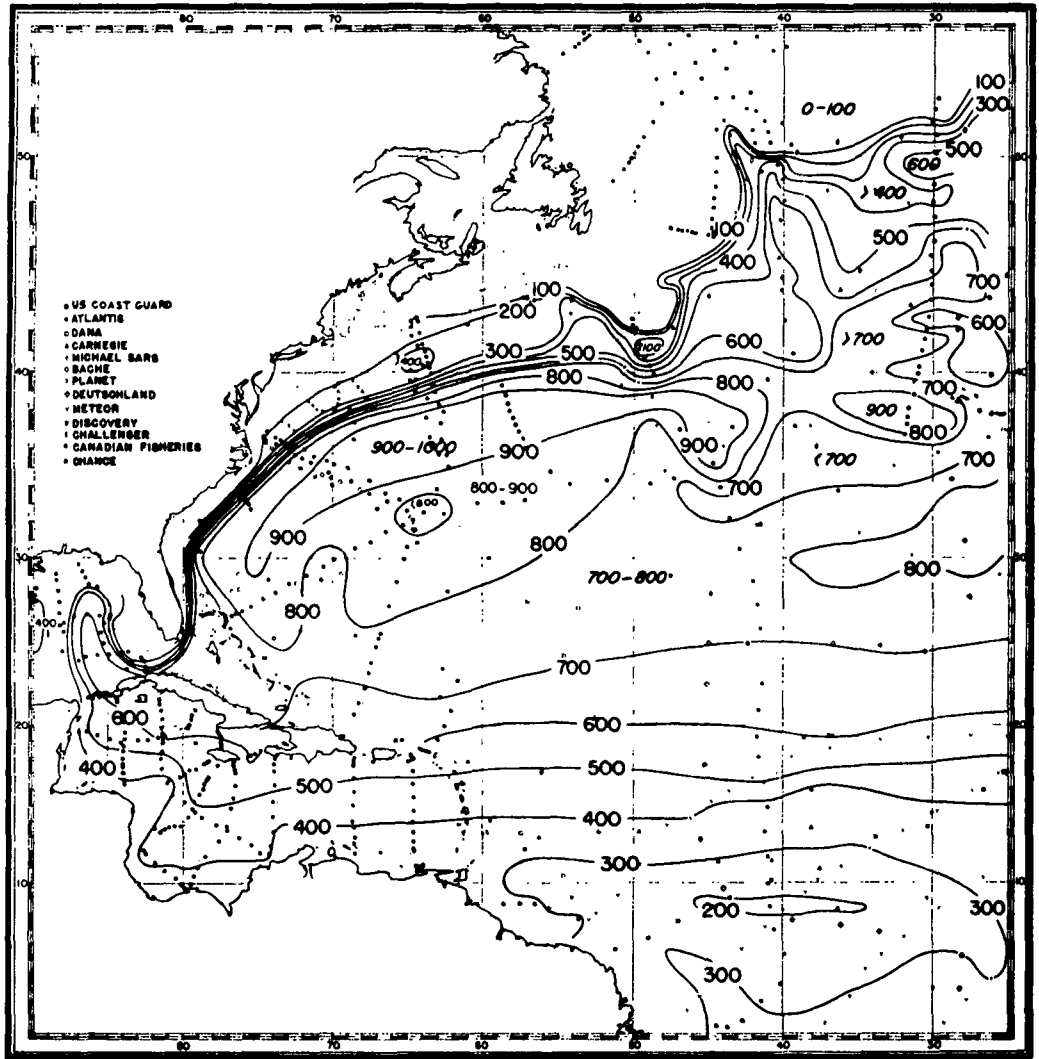


Fig. 4 -- Depth of the 10°C isothermal surface in the western North Atlantic (in meters)⁽²⁾

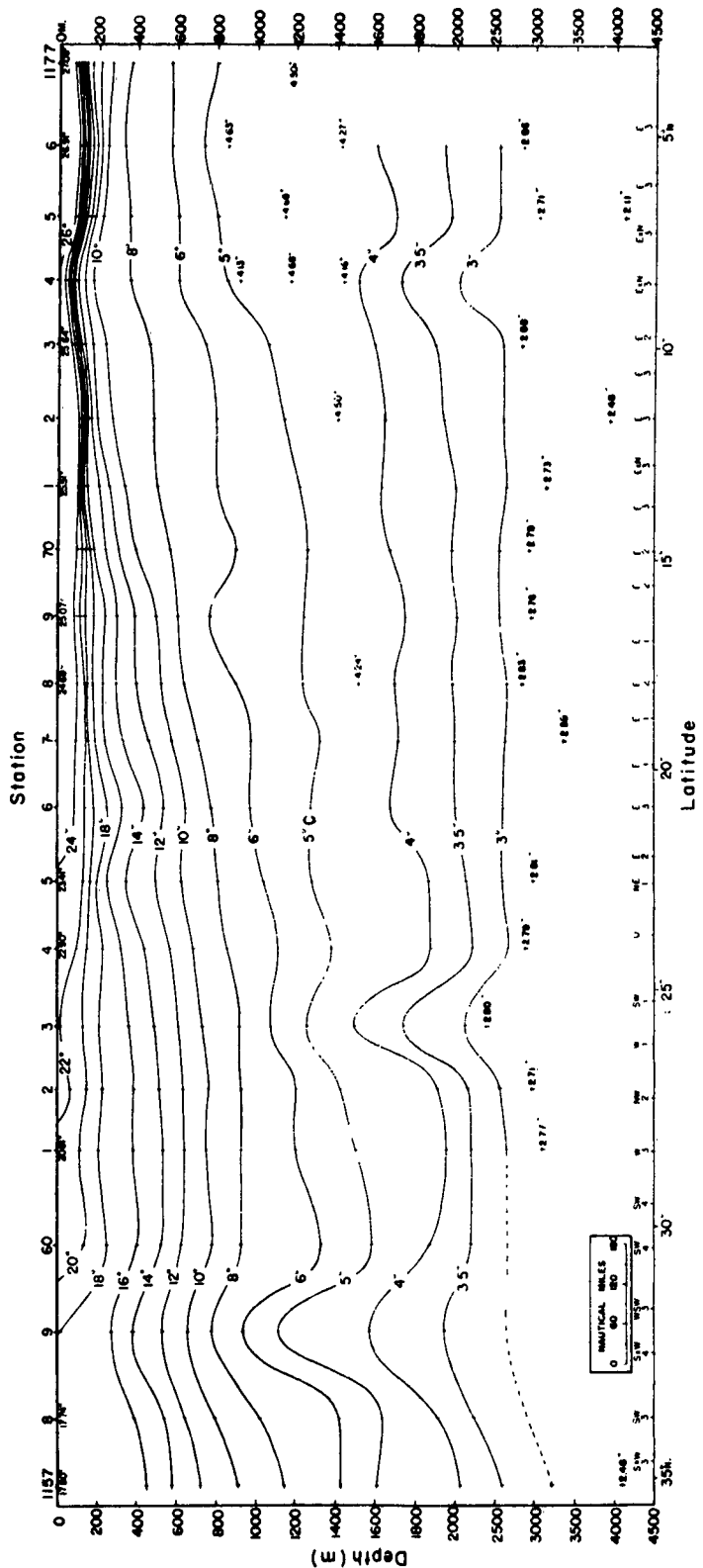


Fig. 5 -- North-South temperature section through the Caribbean, indicating approximate constancy of potential vorticity

He considers the cross section of the stream as illustrated in Fig. 6. There, h is the height of the free surface, D is the thickness from the surface to the 10°C isotherm, g is the acceleration of gravity, ρ is the density (gm/cc), and f is the coriolis parameter. As a basis for the model, we assume the following points:

1. The velocity may be considered to be directed to the north, and $u \frac{\partial u}{\partial x}$ and $v \frac{\partial u}{\partial y}$ are negligible compared with fv and $\frac{\partial p}{\partial x}$.
2. Frictional effects in the water as it flows from the Caribbean to the point of observation are negligible.

Assumption (2) implies assumption (3), which is

3. The potential vorticity in a line of constant density in a cross section is some known function which can be evaluated near the source of the stream.

Assumption (1) is not serious, and the errors it introduces will be shown to be negligible. Assumptions (2) and (3) are mostly to be justified by the results, although some discussion of them will be given.

The conservation of potential vorticity is briefly derived in Appendix B. It says that if water flows from point to point in a layer of constant density, and if there are no forces, whose curl does not vanish, acting on the water, then, along streamlines

$$\frac{f + \zeta}{D} = \text{constant}$$

where

$$\zeta = \frac{\partial v}{\partial x} - \frac{\partial u}{\partial y}$$

$$f = 2\Omega \sin \theta$$

Ω = angular velocity of the earth

θ = latitude

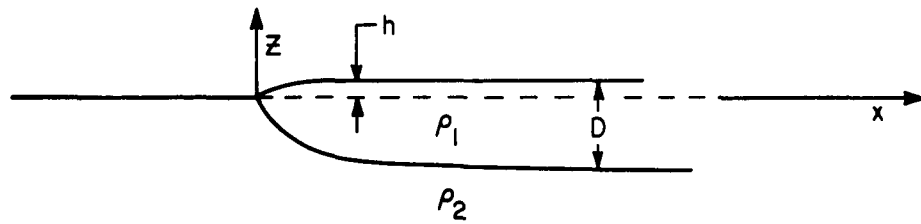


Fig. 6 -- Stommel's one-layer Gulf Stream model
(velocity is directed into the paper)

Stommel's model of the Gulf Stream then assumes that v and $\frac{\partial v}{\partial x}$ vanish far to the right of the intersection of the 10°C isotherm with the surface. Then, making assumption (3) in the form of assuming that the potential vorticity in the layer above the 10°C isotherm is constant in the interior, we set it equal to $\frac{f}{D_0}$. Therefore, across the stream we have

$$\frac{f + \frac{\partial v}{\partial x}}{D} = \frac{f(y)}{D_0(y)} \quad (1)$$

As to the justification for assumption (3) in this particular case, we first quote from Stommel.

The justification for applying the simple model described rests on the observed fact that in the central Atlantic between 10° and 35° N latitude, the potential vorticity of the top isothermal layers ($> 10^{\circ}\text{C}$) is remarkably constant. Suppose, for example, that the quantity D_0 is the thickness of the layer between the sea surface and the 10°C isothermal surface. The depth of the 10°C isotherm is shown in Fig. 66 [our Fig. 4]. Since the relative vorticity in central oceanic regions is small, the reader may compute f/D_0 for the region between 10° and 35°N and convince himself that over this large part of the ocean the potential vorticity, so defined is actually uniform and nearly constant. (1)

Now, since this is the region from which all the water in the stream is drawn, according to the transport lines of Iselin, it is clear why we may set the potential vorticity equal to a constant across the stream even though it is dynamically a constant only along stream lines. Still, if the water because of turbulent viscosity did not retain its original potential vorticity as it traveled along the stream lines, its value might be changed from its constant value by the time it arrived at the observation point, and the theory could not apply.

Next, we assume a level of no motion below the 10°C isotherm. So we have, referring to Fig. 6

$$(D - h) \rho_2 = D\rho_1$$

The pressure gradient in the upper layer due to the elevation of the free surface is

$$\frac{\partial P_1}{\partial x} = g\rho_1 \frac{\partial h}{\partial x}$$

And, by assumption (1), all nonlinear $(\underline{u} \cdot \nabla)\underline{u}$ are small and the geostrophic equation is valid.

$$fv = \frac{1}{\rho} \frac{\partial P_1}{\partial x}$$

Combining the three equations above, we get

$$fv = \frac{1}{\rho} \frac{\partial D}{\partial x} \quad (2)$$

where

$$g' = g \frac{\rho_2 - \rho_1}{\rho_2}$$

Combining Eqs. (1) and (2), we get

$$\frac{\partial^2 D}{\partial x^2} = \frac{1}{\lambda^2} (D - D_0) \quad (3)$$

where

$$\lambda^2 = \frac{g'D_0}{f^2}$$

Imposing the condition that D goes to D_0 and v goes to 0 at infinity, and $D = 0$ at $x = 0$, we find

$$D = D_0 (1 - e^{-x/\lambda}) \quad \text{and} \quad v = \sqrt{g'D_0} e^{-x/\lambda} \quad (4)$$

If we set $D = 800$ m and $g' = 2 \times 10^{-3}$ m/sec², then we get a maximum velocity of 4 m/sec. If we take f at 35°N, we get $\lambda = 48.6$ km.

It is of interest to note here that Iselin's cross section gives λ approximately equal to 90 km.

Extending the One-Layer Model--Caribbean Potential Vorticity

It is natural to try to get more detailed models of the Gulf Stream by elaborating on this simple model of Stommel's. This is what we shall do in the next few pages. Before making these extensions, it is necessary to discuss assumption (3) in somewhat more detail. We have seen that the potential vorticity of the water above the 10°C isotherm in the Caribbean is nearly constant; this gave us the justification for the simple one-layer model. Now, if we are to do many-layered models, or even a continuous model, we must assume that each layer considered has constant potential vorticity in the Caribbean. From Fig. 5 we can see that this is approximately true for the water between the 24°C and 10°C isotherms. However, because the thickness of the layers is approximately constant below the 10°C isotherm, the potential vorticity increases in this layer as we move to the north. But even this will be changed by only a factor of about two for the source region considered, so that it still may be profitable for qualitative considerations to extend the model below the depth of the 10°C isotherm. It is also of interest to note that since we will actually use density and not temperature as our marking property, the constancy of potential vorticity in the Caribbean is not as good for Iselin's density cross sections as for his temperature cross sections.

TWO-LAYER MODELS

Establishing the Models

Making use of the above comments, we shall now consider two-layer models of the Gulf Stream, as illustrated in Fig. 7. In this model (essentially Stommel's model split in two) we have two layers of equal thickness of 400 m at infinity, but of differing densities, ρ_1 and ρ_2 .

A level of no motion below D_2 gives the requirement

$$(D_2 - h_2) \rho_3 = D_1 \rho_1 + D_2 \rho_2$$

and we see that

$$h_1 + h_2 = D_1$$

where h_1 and h_2 represent elevations or depressions of their respective boundaries from the free-equilibrium height to the west.

For the pressure variations we have

$$\frac{\partial p_1}{\partial x} = g \rho_1 \frac{\partial h_1}{\partial x} \quad \frac{\partial p_2}{\partial x} = g \rho_1 \frac{\partial h_1}{\partial x} + g (\rho_2 - \rho_1) \frac{\partial h_2}{\partial x}$$

Combining these slightly more complicated equations (as was done in Stommel's model) with the approximation

$$\frac{\rho_2 - \rho_1}{\rho_2} \cong \frac{\rho_2 - \rho_1}{\rho_3} \quad \text{etc.}$$

we get

$$v_1 = \frac{g}{f} \left[\Delta \rho_1 \frac{\partial D_1}{\partial x} + \Delta \rho_2 \frac{\partial D_2}{\partial x} \right] \quad (5a)$$

$$v_2 = \frac{g}{f} \left[\Delta \rho_2 \frac{\partial D_1}{\partial x} + \Delta \rho_2 \frac{\partial D_2}{\partial x} \right] \quad (5b)$$

where

$$\Delta \rho_i = \frac{\rho_3 - \rho_i}{\rho}$$

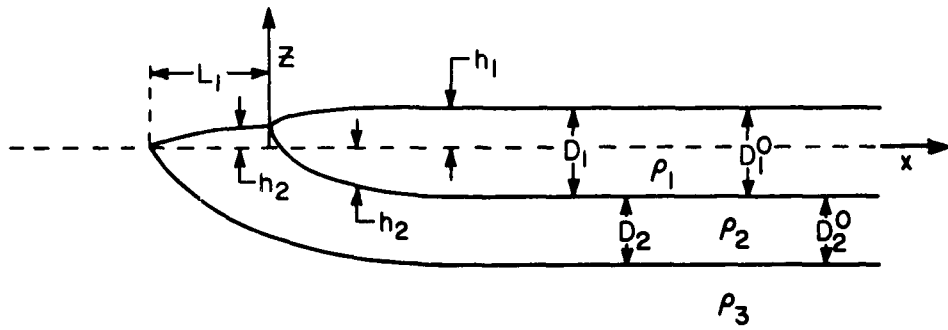


Fig. 7 -- Schematic of two-layer models of the Gulf Stream

We also get

$$\gamma \frac{\partial^2 D_1}{\partial x^2} + \frac{\partial^2 D_2}{\partial x^2} = \frac{1}{\beta \lambda^2} (D_1 - D_1^0) \quad (6a)$$

$$\frac{\partial^2 D_1}{\partial x^2} + \frac{\partial^2 D_2}{\partial x^2} = \frac{1}{\lambda^2} (D_2 - D_2^0) \quad (6b)$$

where

$$\lambda^2 = \frac{g \Delta \rho_2 D_1^0}{f^2}$$

$$\beta = \frac{D_1^0}{D_2^0}$$

$$\gamma = \frac{\Delta \rho_1}{\Delta \rho_2}$$

These equations hold wherever we have two layers. When there is only one layer, as to the left of $x = 0$ in Fig. 7, we need only use the uncomplicated one-layer equations to obtain the solution for that region.

It is necessary to solve the system of coupled simultaneous equations and then to impose boundary conditions.

The solution of the homogeneous equations is of the form

$$D_1 = a_1 e^{\alpha_1 x} + a_2 e^{-\alpha_1 x} + a_3 e^{\alpha_2 x} + a_4 e^{-\alpha_2 x} \quad (7a)$$

$$D_2 = b_1 e^{\alpha_1 x} + b_2 e^{-\alpha_1 x} + b_3 e^{\alpha_2 x} + b_4 e^{-\alpha_2 x} \quad (7b)$$

where the α 's satisfy the determinantal requirement

$$\begin{vmatrix} \gamma \alpha^2 - \frac{1}{\beta \lambda^2} & \alpha^2 \\ \alpha^2 & \alpha^2 - \frac{1}{\lambda^2} \end{vmatrix} = 0$$

or

$$(\gamma - 1) \alpha^4 - \frac{1}{\lambda^2} \left(\gamma + \frac{1}{\beta}\right) \alpha^2 + \frac{1}{\beta \lambda^4} = 0 \quad (8)$$

To determine the connections between the eight unknown coefficients, a_i , b_i , we substitute the above solutions into either Eq. (6a) or (6b) and set the coefficient of each exponential equal to zero. For the coefficients of the negative exponentials, we get

$$a_2 = \frac{\lambda^{\frac{1}{2} - \alpha_1^2}}{\alpha_1^2} b_2 \quad a_4 = \frac{\lambda^{\frac{1}{2} - \alpha_2^2}}{\alpha_2^2} b_4$$

If we also insist that the solution remain finite at infinity, we get

$$a_1 = b_1 = a_3 = b_3 = 0$$

Then the solution in the region of two layers is, adding the particular solutions D_1^0 and D_2^0

$$D_1 = b_2 \frac{\lambda^{\frac{1}{2} - \alpha_1^2}}{\alpha_1^2} e^{-\alpha_1 x} + b_4 \frac{\lambda^{\frac{1}{2} - \alpha_2^2}}{\alpha_2^2} e^{-\alpha_2 x} + D_1^0 \quad (9a)$$

$$D_2 = b_2 e^{-\alpha_1 x} + b_4 e^{-\alpha_2 x} + D_2^0 \quad (9b)$$

If we use the single-layer equations for the bottom layer, the solution to the left of $x = 0$ is, if we impose $D = 0$ at $x = -L_1$

$$D_2 = b_0 \left[e^{-x/\lambda} - e^{-(2L_1 + x)/\lambda} \right] + D_2^0 \left[1 - e^{-(L_1 + x)/\lambda} \right] \quad (10)$$

Now that we have the solutions in the various regions, we must join them by appropriate boundary conditions. We shall always impose continuity of layer thickness and of velocity at the boundaries. It should be noted that because potential vorticity is conserved across the stream,

$\frac{\partial v}{\partial x}$ is automatically continuous across the boundaries. Finally, by comparing Eqs. (2) and (5b), we see that the continuity of v guarantees the smoothness of $(D_1 + D_2)$, which is the boundary line between ρ_2 and ρ_3 .

Examples of Two-Layer Models

For our first model, let us suppose that the bottom 400-m layer never rises to the surface to the left of $x = 0$ and that it goes to its asymptotic value of 400 m. Then, if we prescribe as typical values

$$\begin{aligned} \Delta\rho_1 &= 2 \times 10^{-3} & \Delta\rho_2 &= 10^{-3} & D_1^0 &= D_2^0 &= 400 \text{ m} \\ f &= 10^{-4} \text{ sec}^{-1} & g &= 10 \text{ m/sec}^2 & \lambda &= 20 \text{ km} \end{aligned}$$

we get as a solution the six parts of Eq. (11)

$$\begin{aligned} D_2^L &= D_2^0 \left[1 + 0.236 e^{x/\lambda} \right] & (m) \\ D_2^R &= D_2^0 \left[1 + 0.618 e^{-1.618x/\lambda} - 0.382 e^{-0.618x/\lambda} \right] \\ D_1^R &= D_1^0 \left[1 - 0.618 e^{-0.618x/\lambda} - 0.382 e^{-1.618x/\lambda} \right] & (11) \\ v_2^L &= 0.472 e^{x/\lambda} & (m/sec) \\ v_2^R &= 1.236 e^{-0.618x/\lambda} - 0.764 e^{-1.618x/\lambda} \\ v_1^R &= 2.00 e^{-0.618x/\lambda} + 0.472 e^{-1.618x/\lambda} \end{aligned}$$

This is graphed in Fig. 8.

The maximum velocity is 2.47 m/sec; there is a velocity to the left of $x = 0$ which was not found in Stommel's model, and the maximum velocity in the lower layer is displaced 9.62 km to the right. This corresponds to a slope of the axis of maximum velocity of between 1/25 to 1/50.

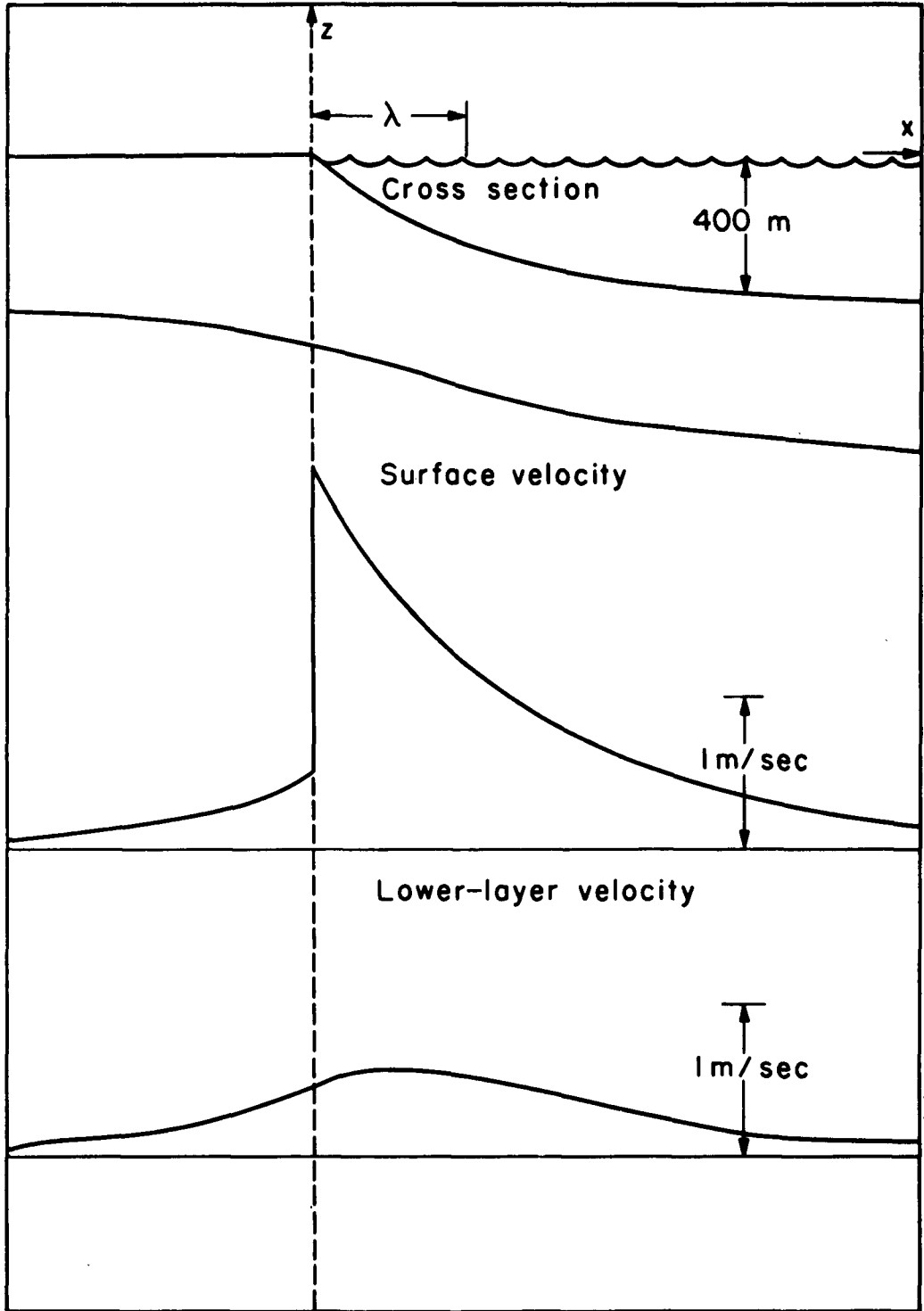


Fig. 8 -- Two-layer model where lower layer does not rise to the surface, showing the recession of the axis of maximum velocity with depth

For our next model, we make the upper layer a warm core because we anticipate that this will give a countercurrent. However, it is difficult to determine the core's potential vorticity, since none of its density lines extend to infinity on the right where the water is at rest. Now, Fig. 9 shows the density structure which we wish to model. The experimental section is taken from Worthington,⁽⁴⁾ his Fig. 4.

From the fact that λ is typically of the order of 40 km, we anticipate that in this model $v = 0$ in the middle of the warm core. Therefore, assuming that this layer came from a region of uniform potential vorticity, we may set the potential vorticity in this region equal to f/D_0 , where D_0 is the observed thickness of the core at its middle (equal to 125 m in this case). If we knew where this water came from, we could observe the water in the source region and calculate its potential vorticity. Then, as a solution, we get Eq. (12), which is graphed in Fig. 10. It is seen that indeed we do get a countercurrent and that the axis of maximum countercurrent velocity recedes westward under the stream as one would anticipate. The eight parts of Eq. (12) are

$$\begin{aligned}
 D_2^L &= 39.41 e^{x/\lambda_0} - 53.05 e^{-x/\lambda_0} + 440 & (m) \\
 D_2^R &= 40.48 e^{-\left(\frac{x-200}{\lambda_0}\right)} + 440 \\
 D_2^M &= 128.6 e^{\alpha_1 \left(\frac{x-200}{\lambda_0}\right)} + 115.5 e^{-\alpha_1 x/\lambda_0} & (12) \\
 &- 88.0 e^{\alpha_2 \left(\frac{x-200}{\lambda_0}\right)} - 129.0 e^{-\alpha_2 x/\lambda_0} + 440
 \end{aligned}$$

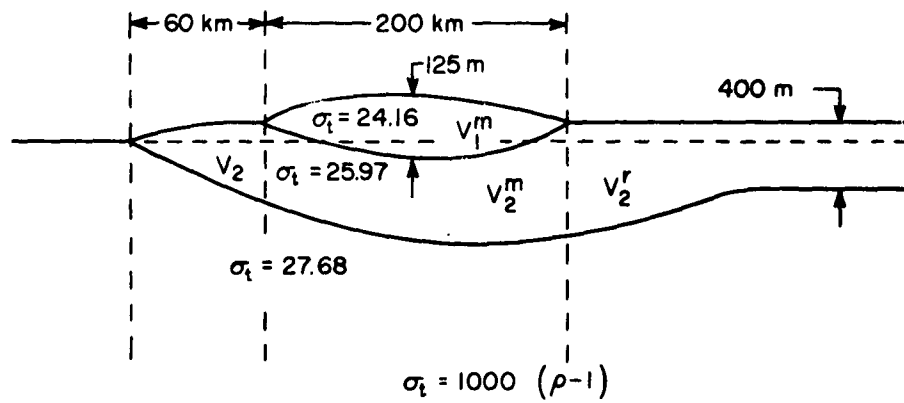


Fig. 9 -- Two-layer model to be solved to give countercurrent⁽⁴⁾

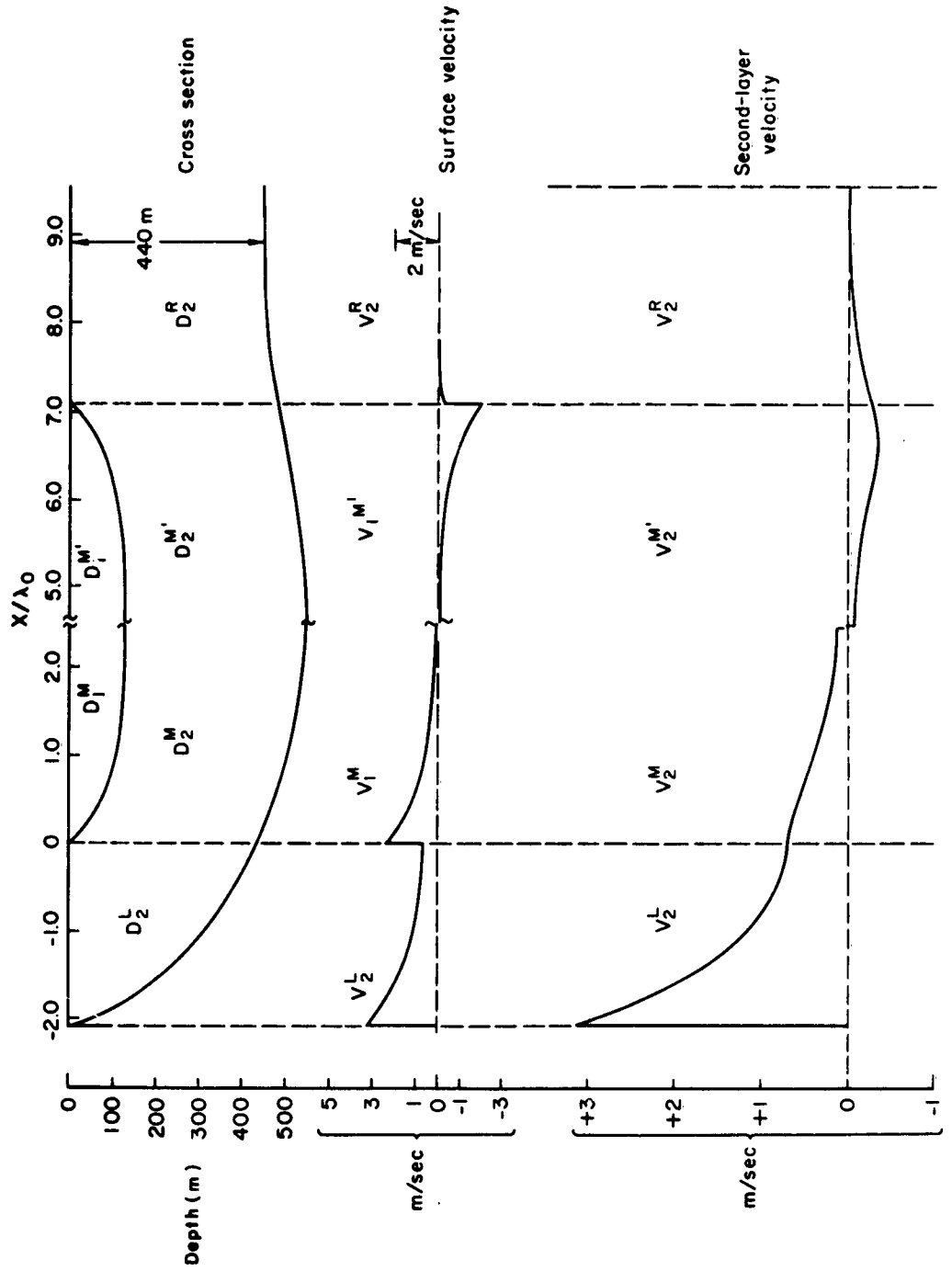


Fig. 10 -- Solution of Fig. 9 from Eq. (12)

$$\begin{aligned}
 D_1^M &= -102.5 e^{\alpha_1 \left(\frac{x-200}{\lambda_0} \right)} - 92.0 e^{-\alpha_1 x / \lambda_0} \\
 &\quad - 22.22 e^{\alpha_2 \left(\frac{x-200}{\lambda_0} \right)} - 32.60 e^{-\alpha_2 x / \lambda_0} + 125 \\
 v_2^L &= 0.296 e^{x/\lambda_0} + 0.398 e^{-x/\lambda_0} \quad (\text{m/sec}) \\
 v_2^R &= -0.304 e^{-\left(\frac{x-200}{\lambda_0} \right)} \\
 v_2^M &= 0.436 e^{\alpha_1 \left(\frac{x-200}{\lambda_0} \right)} - 0.388 e^{-\alpha_1 x / \lambda_0} \\
 &\quad - 0.740 e^{\alpha_2 \left(\frac{x-200}{\lambda_0} \right)} + 1.087 e^{-\alpha_2 x / \lambda_0} \\
 v_1^M &= -1.190 e^{\alpha_1 \left(\frac{x-200}{\lambda_0} \right)} + 1.061 e^{-\alpha_1 x / \lambda_0} \\
 &\quad - 0.880 e^{\alpha_2 \left(\frac{x-200}{\lambda_0} \right)} + 1.291 e^{-\alpha_2 x / \lambda_0}
 \end{aligned} \tag{12}$$

where

$$\lambda_0 = 28.22 \text{ km}$$

$$\alpha_1 = 2.233$$

$$\alpha_2 = 0.8934$$

This result is only semiquantitative, since Fig. 9 is a bad approximation of the true density structure, which has large gradients inside the core.

ROTATION OF CO-ORDINATE SYSTEM TO STREAM AXES

Before moving on to the continuous case, it would be well to verify whether assumption (1) (page 10) can be valid in the case of the Gulf Stream.

Going back to Stommel's model, if we include both north-south and east-west velocities, we have, corresponding to Eq. (1)

$$\frac{f + \frac{\partial v}{\partial x} - \frac{\partial u}{\partial y}}{D} = \frac{f}{D_0}$$

Upon substituting

$$fv = g' \frac{\partial D}{\partial x}$$

$$fu = g' \frac{\partial D}{\partial y}$$

we get

$$\frac{f + g'/f \left(\frac{\partial^2 D}{\partial x^2} + \frac{\partial^2 D}{\partial y^2} \right) - g' \left(\frac{\partial f}{\partial y} / f \right) \frac{\partial D}{\partial y}}{D} = \frac{f}{D_0}$$

Now, the ratio of the third term in the numerator of the left-hand side of the above equation to the other two if the stream is proceeding in a north-westerly direction is approximately

$$\frac{\left(\frac{\partial f}{\partial y} / f \right) \frac{\partial D}{\partial y}}{\frac{1}{f} \frac{\partial^2 D}{\partial y^2}}$$

which, by differentiating Stommel's solution to get approximate values for the derivatives, is of the order $\frac{\lambda}{R}$, where R is the radius of the earth.

Thus, this term may clearly be neglected. Next, it is well known that the Laplacian equation is invariant under co-ordinate rotations. Therefore, in the equation resulting from the above simplification we may rotate the co-ordinate system until the derivative normal to the stream contains all of the numerical magnitude of the Laplacian equation. If we then call this direction "x," we have recovered the original equation.

THE CONTINUOUS CASE

Development of Theory

This discussion follows in broad outline the paper of Rossby.⁽⁵⁾

Let us define a vertical co-ordinate r such that

$$r = \frac{\rho_b - \rho}{\rho_b - \rho_s} \quad (13)$$

where

ρ_s = density at the surface

ρ_b = density at bottom of region of interest

Note that r goes from 0 at the bottom to 1 at the surface. We also define K , a constant, such that

$$K = \frac{\rho_b - \rho_s}{2\rho_b}$$

It follows that

$$\rho = \rho_b(1 - 2Kr)$$

Remembering Eq. (1) for the conservation of potential vorticity, we rewrite it as

$$\frac{\partial v}{\partial x} = f \left(\frac{D - D_o}{D_o} \right)$$

To pass to the continuous case, we replace D by an infinitely thin layer

$$D = + \frac{\partial z}{\partial \rho} d\rho = + \frac{\partial z}{\partial r} dr$$

and get

$$\frac{\partial v}{\partial x} = f \left(\frac{\left(\frac{\partial z}{\partial r} - \left(\frac{\partial z}{\partial r} \right)_o \right)}{\left(\frac{\partial z}{\partial r} \right)_o} \right)$$

We now define $Z_0(r)$ as a function, giving the z co-ordinate, infinitely far to the right, of water with the density co-ordinate r . We can, therefore, rewrite the previous equation as

$$\frac{\partial v}{\partial x} = f \left(\frac{\frac{\partial z}{\partial r} - \frac{\partial Z_0}{\partial r}}{\frac{\partial Z_0}{\partial r}} \right) \quad (14)$$

We should remember at this point that the above equation is for the conservation of potential vorticity; as such, $\frac{\partial v}{\partial x}$ is actually $\frac{\partial v}{\partial x}$ with the density held constant, and so it may be written $\left(\frac{\partial v}{\partial x}\right)_\rho$.

Equation (14) can be rigorously derived as an approximate form for the rigorously derived Eq. (65) in Appendix B.

We now define

$$\Delta = z(r) - Z_0(r)$$

and the equation above becomes

$$\left(\frac{\partial v}{\partial x}\right)_\rho = f \frac{\frac{\partial \Delta}{\partial r}}{\frac{\partial Z_0}{\partial r}} \quad (15)$$

Now the pressure at some depth z is

$$p = \int_z^{\text{surface}} g\rho dz$$

Integrating by parts, we get

$$p = g\rho_s h - g\rho(z)z - \int_{\rho(z)}^{\rho(s)} gz d\rho \quad (16)$$

where

$$\rho(s) = \rho \text{ on surface}$$

$$\rho(z) = \rho \text{ at } z$$

Now, it is easily seen that

$$\left(\frac{\partial p}{\partial x}\right)_z = \left(\frac{\partial p}{\partial x}\right)_\rho + g\rho(z) \left(\frac{\partial z(\rho)}{\partial x}\right)_\rho \quad (17)$$

To obtain the first term on the right-hand side of the above equation, we substitute the derivative of the right-hand side of Eq. (16).

Equation (17) becomes

$$\left(\frac{\partial p}{\partial x}\right)_z = g\rho(s) \left(\frac{\partial h}{\partial x}\right)_\rho - g\rho(z) \left(\frac{\partial z(\rho)}{\partial x}\right)_\rho - \left(\frac{\partial}{\partial x}\right)_\rho \int_{\rho(z)}^{\rho(s)} gz d\rho + g\rho(z) \left(\frac{\partial z(\rho)}{\partial x}\right)_\rho \quad (18)$$

The second and fourth terms cancel, and the third term becomes

$$-gz(s) \frac{\partial \rho(s)}{\partial x} - \int_{\rho(z)}^{\rho(s)} g \frac{\partial z(\rho)}{\partial x} d\rho$$

Now, since

$$z(s) = h, \quad \frac{\partial z(r)}{\partial x} = \frac{\partial \Delta}{\partial x} \quad \text{and} \quad d\rho = -2K\rho_b dr$$

this becomes

$$2K\rho_b g \left\{ h \left(\frac{\partial r(s)}{\partial x}\right) + \int_r^{r(s)} \frac{\partial \Delta}{\partial x} dr \right\}$$

So, finally

$$\left(\frac{\partial p}{\partial x}\right)_z = g\rho(s) \left(\frac{\partial h}{\partial x}\right)_\rho + 2K\rho_b g \left\{ h \frac{\partial r(s)}{\partial x} + \int_r^{r(s)} \frac{\partial \Delta}{\partial x} dr \right\} \quad (19)$$

Note that Eq. (19) is also correct if we replace x with y. This will be of use later in this Memorandum in an analysis of the Cromwell Current.

At this point, it is convenient to introduce a level of no motion at some arbitrary great depth. For convenience we take it to be the greatest depth attained by ρ_b . If this level is taken to be the zero point for the z-axis, then we have

$$\int_{z(r(b))}^{z(r(s))} g\rho dz + \rho_b gz(r(b)) = \text{constant} \quad (20)$$

Integrating by parts we get

$$0 = \rho(s) gz(r(s)) - \rho(b) gz(r(b)) - \int_{r(b)}^{r(s)} gzd\rho + \rho(b)gz(r(b))$$

Canceling the second and fourth terms and then taking $\left(\frac{\partial}{\partial x}\right)_\rho$ gives

$$\rho(s)g \frac{\partial z(r(s))}{\partial x} + 2Kg h_o \left\{ z(r(s)) \frac{\partial r(s)}{\partial x} + \int_{r(b)}^{r(s)} \frac{\partial \Delta}{\partial x} dr \right\} = 0$$

Substituting this in Eq. (19) cancels the unwanted first and second terms, and adding the integrals gives

$$\left(\frac{\partial p}{\partial x}\right)_z = -2Kg\rho(b) \int_{r(b)}^r \frac{\partial \Delta}{\partial x} dr \quad (21)$$

and, finally, the geostrophic relationship gives

$$v = -\frac{2Kg}{f} \int_{r(b)}^{r(z)} \frac{\partial \Delta}{\partial x} dr \quad (22)$$

This, then, is the formula which we may use to calculate the velocity when we have calculated the final $\Delta(x,r)$.

Taking the derivative of Eq. (22) we find

$$\left(\frac{\partial v}{\partial x}\right)_\rho = -\frac{2Kg}{f} \int_{r(b)}^r \frac{\partial^2 \Delta}{\partial x^2} dr \quad (22a)$$

and then

$$\frac{\partial}{\partial r} \left(\frac{\partial v}{\partial x}\right)_\rho = -\frac{2Kg}{f} \frac{\partial^2 \Delta}{\partial x^2} \quad (23)$$

But if we differentiate, with respect to r , Eq. (14) for the conservation of vorticity, we may set the right-hand side equal to the right-hand side of Eq. (23), and upon rearrangement of terms there results finally, with primes indicating differentiation with respect to r

$$\frac{\partial \Delta}{\partial r^2} + \frac{2KgZ'_0}{f^2} \frac{\partial^2 \Delta}{\partial x^2} - \frac{Z''_0}{Z'_0} \frac{\partial \Delta}{\partial r} = 0 \quad (24)$$

This is the final equation. It now becomes necessary to define the region in which it is to be solved. Since r is our vertical coordinate, the region is bounded below by $r = 0$. On the surface far to the right $r = 1$, but as we move left, we see from Fig. 1 that the lines of density come to the surface and thus the surface value of r must decrease. Therefore, the region in which Eq. (24) is to be solved must look something like Fig. 11.

It should be remembered here that while the v 's in Eqs. (23) and (14) are both in the geometrical co-ordinate system, Eq. (14) is only an approximation to Eq. (65) in Appendix B, and therefore Eq. (24) is also an approximation.

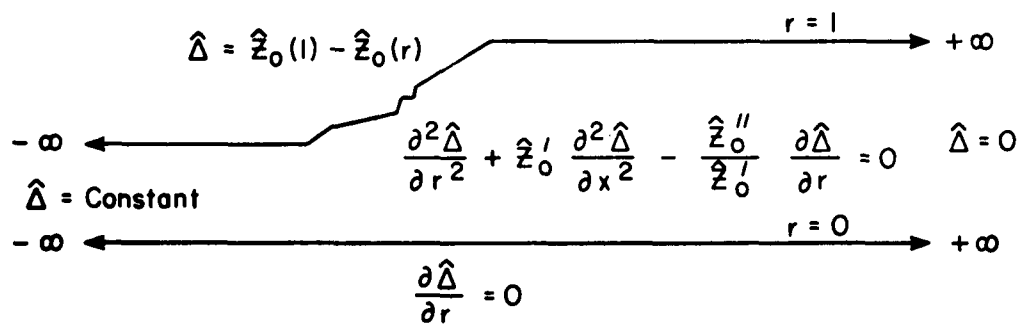


Fig. 11 -- Boundary of the region to be solved in (x,r) co-ordinates for Eq. (24)

Boundary Conditions

Next, we consider the boundary conditions which must be satisfied. Clearly, to the far right the boundary condition must be $\Delta = z(r) - Z_0(r) = 0$. Now, far to the left, if potential vorticity has been conserved and the velocity vanishes, the profile of density can only have been displaced upward, and so $\Delta = \text{constant}$. In between, on the free surface, we see that where the density r reaches the surface, the boundary condition states that Δ must equal the distance which that density line has risen. That is, $\Delta = Z_0(1) - Z_0(r) = h$, where h is the height of the free surface. But the height of the free surface is negligible compared to $Z_0(1) - Z_0(r)$, and therefore the surface boundary condition is $\Delta = Z_0(1) - Z_0(r)$.

There remains only the bottom boundary condition. From Eq. (22) we see that the velocity for $r = r(b)$ is zero. This is true all along the line of constant density, $r = r(b)$. From Eq. (22a) we also see

$$\left(\frac{\partial v}{\partial x}\right)_{\rho=\rho(b)} = 0$$

But this implies by Eq. (14) that $\frac{\partial \Delta}{\partial r} = 0$. Therefore, the boundary condition on the bottom is

$$\frac{\partial \Delta}{\partial r} = 0 \tag{25}$$

For purposes of computation it is convenient to introduce dimensionless variables

$$\begin{aligned} \hat{x} &= \frac{x}{\sqrt{\frac{2Kgh_0}{f^2}}} & \hat{v} &= \frac{v}{\sqrt{2Kgh_0}} \\ \hat{\Delta} &= \Delta/h_0 & \hat{z}_0 &= z_0/h_0 \end{aligned} \tag{26}$$

In terms of these new variables, Eqs. (22) and (24) become

$$\hat{\psi} = - \int_{r(b)}^r \frac{\partial \hat{\Delta}}{\partial x} dr \quad (27)$$

$$\frac{\partial^2 \hat{\Delta}}{\partial r^2} + \hat{Z}'_0 \frac{\partial^2 \hat{\Delta}}{\partial x^2} - \frac{\hat{Z}''_0}{\hat{Z}'_0} \frac{\partial \hat{\Delta}}{\partial r} = 0$$

The nondimensional problem to be solved is sketched in Fig. 11. It is to be noted that with the exception of the core, the data necessary for solution comprise only the density gradients on the surface to give the surface profile and boundary condition, and the density in vertical sections at infinity to the right to give Z'_0 and Z''_0 .

Solution for Continuous Case

Analytical Model. It is of interest now to obtain the simplest possible analytical solution for the continuous case. We consider a linear density gradient in which the entire field of variable density comes to the surface at one point. To see how we shall represent this, consider the problem given by the dotted line in Fig. 12. Here the lines of constant density come to the surface linearly over a small, finite distance. Along this line, $\hat{\Delta}$ is as seen in the projection on the left. If now we pass to the limit where the small finite distance goes to a point, we may consider that the $\hat{\Delta}$ projection remains unchanged. In the interior of the resulting region, signified by the solid line, we have a simple Laplace equation, and on the boundary, simple conditions. This problem is easily solved, and the solution is

$$\hat{\Delta} = \frac{8}{\pi} \sum_{n=1}^{\infty} \frac{1}{(2n-1)^2} \cos \left[\frac{(2n-1)\pi r}{2} \right] e^{-\frac{(2n-1)\pi x}{2}} \quad (28)$$

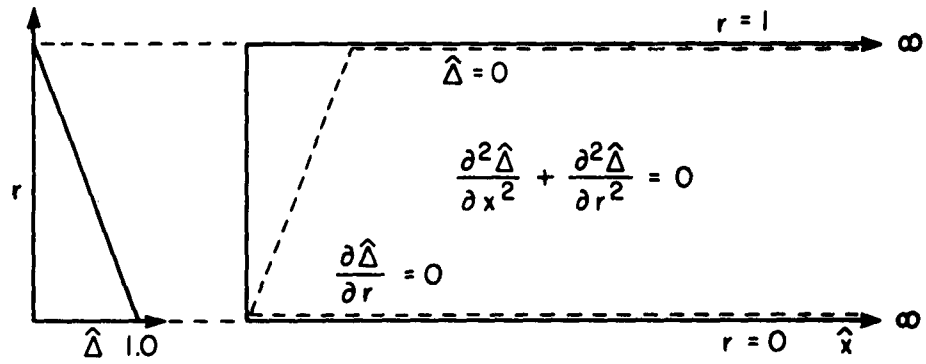


Fig. 12 -- Solution in (x,r) co-ordinates for a linear-density-gradient Gulf Stream

Through Eq. (27) the velocity is

$$\hat{v} = \frac{8}{\pi} \sum_{n=1}^{\infty} \frac{1}{(2n-1)^2} \sin \left[\frac{(2n-1)\pi x}{2} \right] e^{\frac{-(2n-1)\pi z}{2}} \quad (29)$$

A plot of this solution is seen in Fig. 13, where the lines of constant density and velocity are drawn and also a line showing the axis of maximum velocity with depth. The mean slope of the axis of maximum velocity is, in dimensionless co-ordinates, about 1/1.27. The theory naturally fails at the surface at $x = 0$ because of the infinite density gradient and at the bottom because we have placed the level of no motion at too shallow a depth to keep from straining the linear-density-gradient approximation. The failure in the graph of the bottom dotted line to come to the surface shows the effect of plotting only three terms of the series. The ratio of the vertical scale to the horizontal scale is

$$\sqrt{\frac{D_o}{\frac{2KgD_o}{f^2}}} = f \sqrt{\frac{D_o}{g'}}$$

We shall use somewhat more precise constants to extract the most possible from the theory. From Fig. 1 we pick

$$\begin{aligned} D_o &= 900 \text{ m} \\ f &= 0.81 \times 10^{-4} \text{ sec}^{-1} \\ \frac{\Delta \rho}{\rho} &= 0.8 \times 10^{-3} \end{aligned}$$

We find the slope of maximum velocity to be 1/46.5.

Since the maximum nondimensional velocity is 0.743, we find the maximum velocity to be 1.99 m/sec. Finally, we find $\lambda = 33.1$ km. A plot of the nondimensional surface velocity is also seen in Fig. 13.

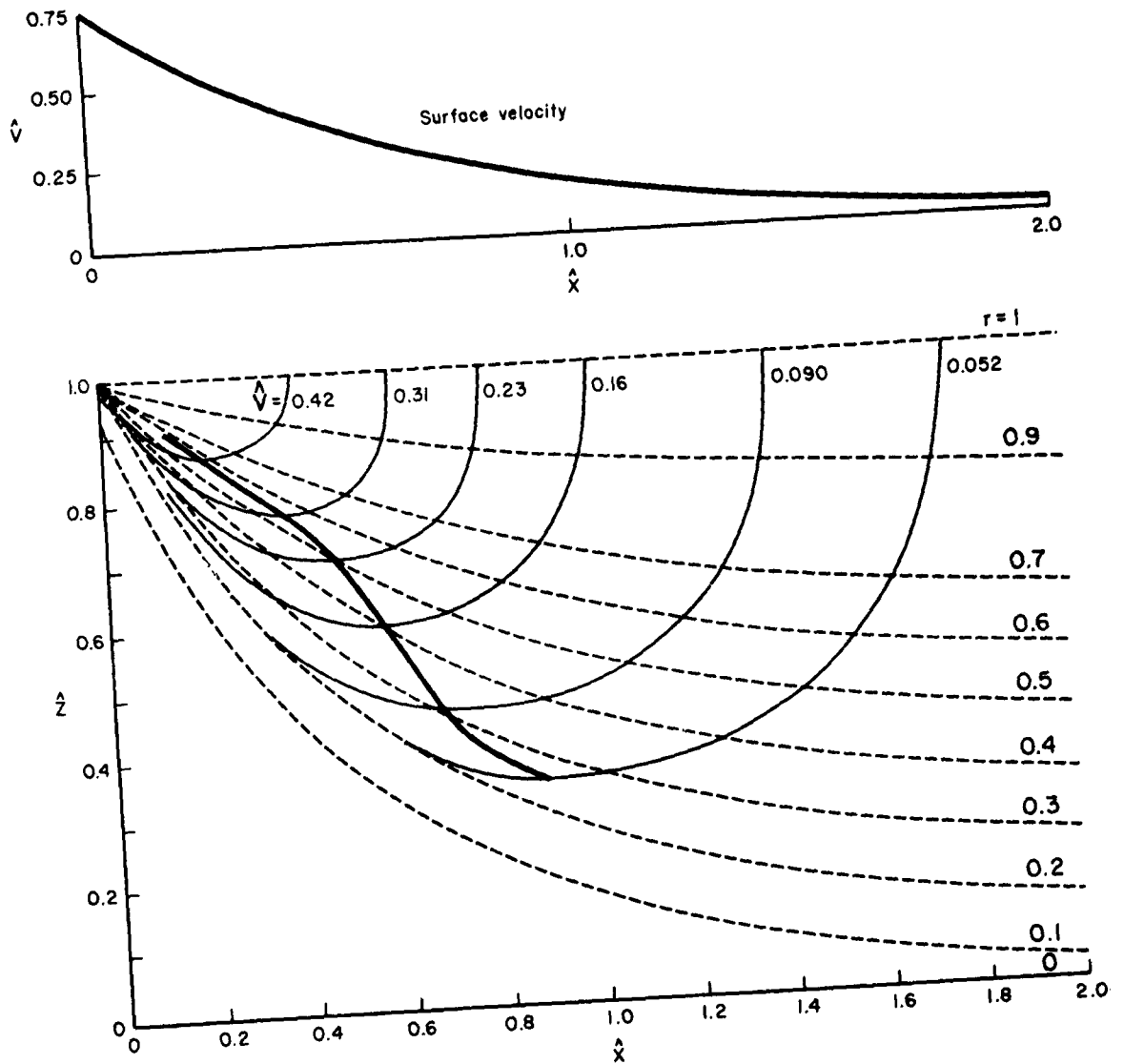


Fig. 13 -- Solution of Fig. 12 in (x,r) co-ordinates

Finally, to extract the greatest possible amount of information from Eq. (24), a numerical solution was made. The left-hand edge was taken as Station 1231 in Fig. 1 and the right-hand edge taken near Station 1223. The region in which Eq. (24) is to be solved in (x,r) coordinates is shown in Fig. 14. Note the large "warm-core" peak on the top of which we find r values of 1.83. This is to be compared with the value of 1.00 for r at infinity on the right. In this core, just as in the core of the two-layer model of the Gulf Stream previously solved, it is necessary to specify the potential vorticity. This is done rather arbitrarily by assuming that in the core, $\frac{\partial v}{\partial x} = 0$ directly under the peak. Thus, this gives the potential vorticity in the core as f/Z'_p , where $Z'_p = Z'$ is just at the peak. Notice that this assumption is contradicted by the results of the computation which give $\frac{\partial v}{\partial x} \neq 0$. We could undoubtedly arrive at a consistent set of values in the core by iteration, but they would not alter the qualitative results except by smoothing out the gradients near the peak. The vertical line under the peak is now regarded as another line of origin just like a vertical line at infinity in the east, from which we measure Δ for the water in the core. Now it is clear that adding a constant number to all Δ above some given r cannot change the velocity structure. It is equally clear that in the numerical solution it will be necessary to have Δ be a continuous function in the interior. Therefore, all the mesh points beneath the highest point in the core must and may have the same value of Δ as the line of greatest r which manages to pass beneath the peak and extend to infinity on the right. If this value of r , forming the bottom of the core, is r_0 , then the constant value of Δ mentioned above is seen to be $Z(x_p, r_0) - Z_0(r_0) = \Delta_0$, where x_p is the x co-ordinate of the peak. This value of Δ_0 must

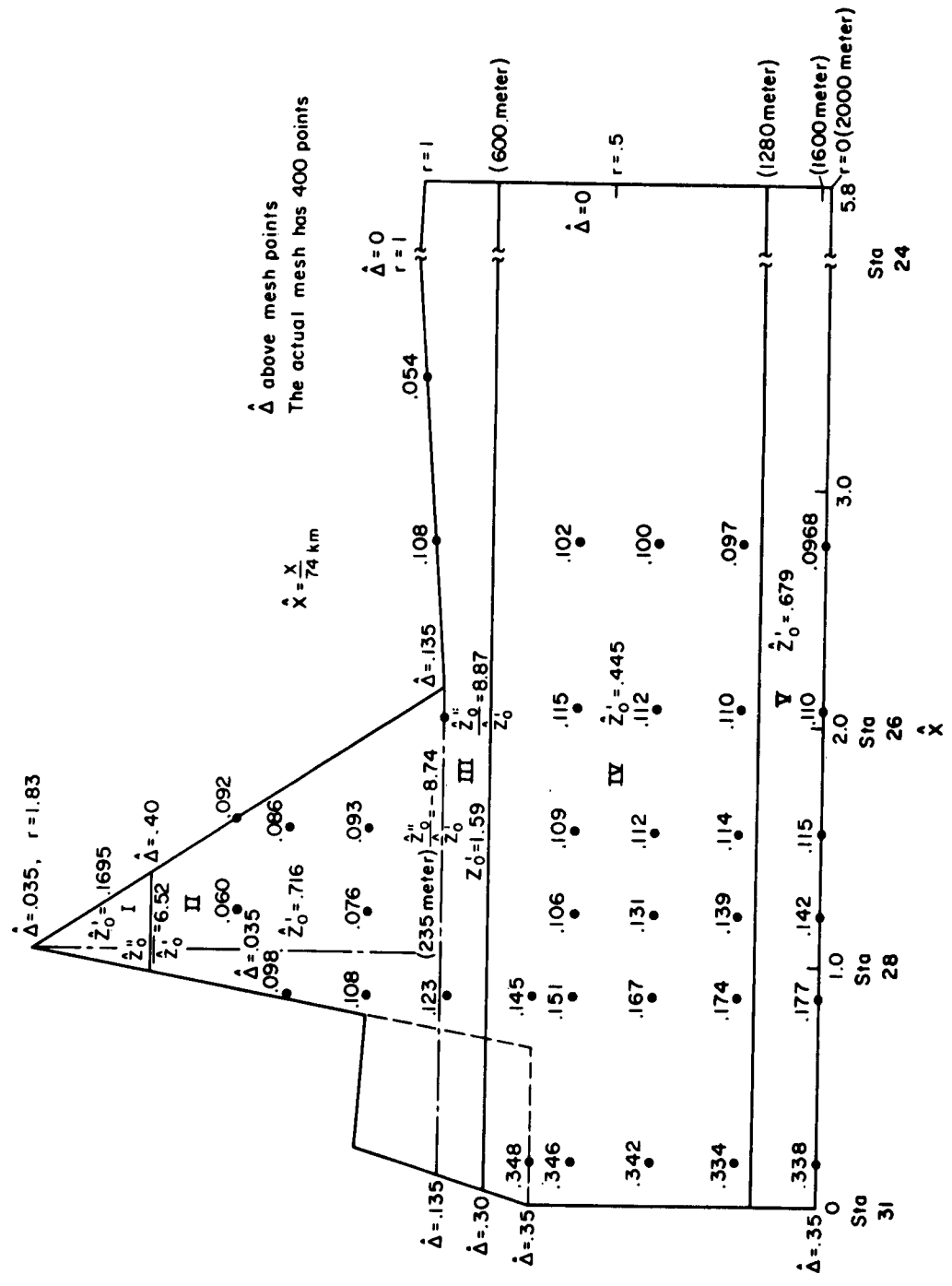


Fig. 14 -- Final Gulf-Stream problem to be solved in (x,r) co-ordinates

then be given to each point beneath the peak. To obtain the surface boundary condition for densities within the core, we add to this constant value the distance which that density line must come up to reach the surface. Note that the many arbitrary elements in this treatment of the core are noted in the two-layer core solution, page 21.

The density structure in Iselin's section at Station 1223 on the east is shown in Fig. 15. This density structure was approximated by the three straight lines as shown. These straight lines gave the value of Z'_0 except at the intersections. If a mesh point in the numerical solution is close to such an intersection, then the value of Z'_0 is taken as the mean of the two on either side. Also, in the equation at such a point, the third term of Eq. (24) comes into play. To evaluate Z''_0 , the difference of the Z'_0 above and below were divided by what seemed, on inspection of the actual graph of density versus depth, to be the proper value of δr . To obtain Z'_0 in the core, the graph of density in Iselin's Station 1228 down to 200 m as shown in Fig. 16 was used. By the above procedure we obtained the coefficients of Eq. (24), the region in which it is to be solved, and the boundary conditions.

Suppose that we construct a mesh for the numerical solution of the problem and that there are a total of n mesh points including the interior and the boundary. If we then express Eq. (24) in finite difference form, then we have n equations of the form

$$\sum_j a_{lj} u_j = \sum_r c_{lr} b_r$$
$$l = 1, 2, \dots, n$$

where u_j represents the unknown values in the interior, and b_r , the known values on the boundary; the a 's and c 's are known coefficients. Since

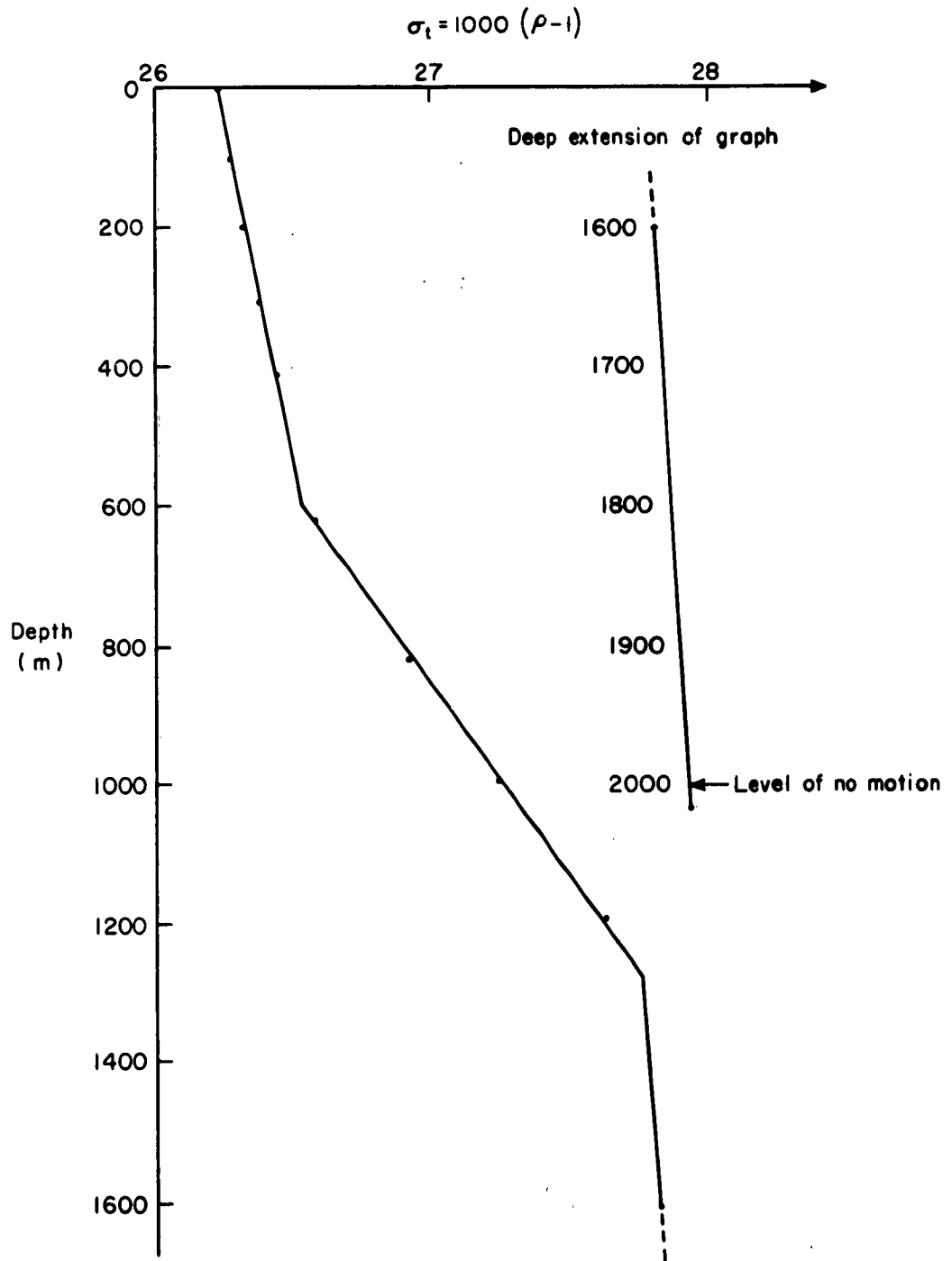


Fig. 15 -- Density structure at Station 1223 in Fig. 1

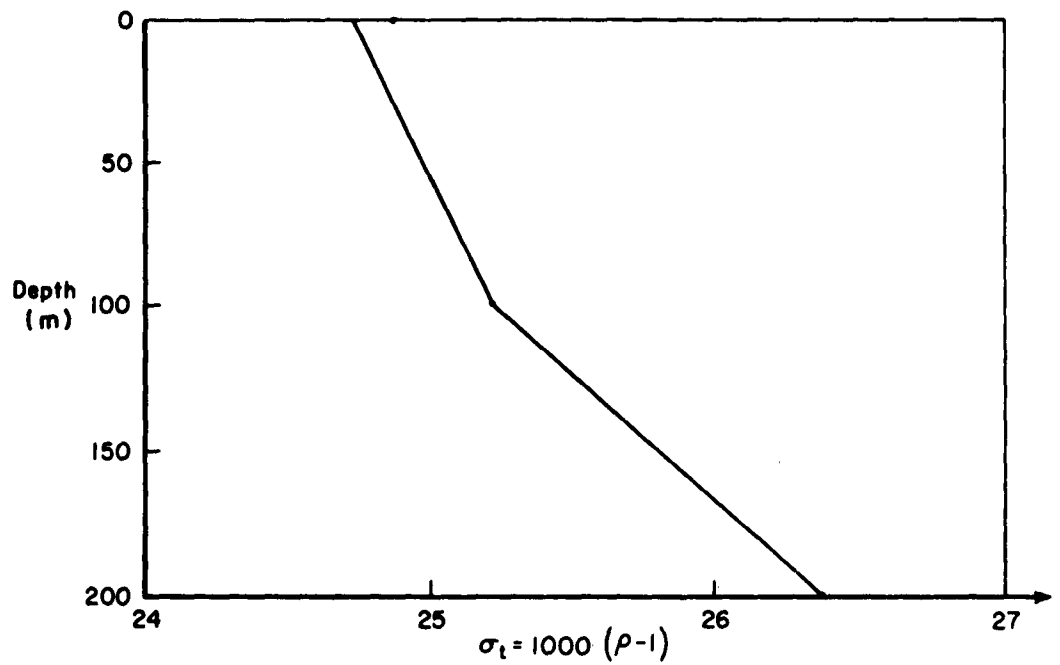


Fig. 16 -- Density structure at Station 1228 in Fig. 1

the a's, b's, and c's are all known, then for each l the right-hand side is just a number, and we may write Eq. (29) as

$$\sum a_{lj} u_j = d_l \quad l = 1, 2, \dots, n \quad (30)$$
$$\vec{A} \vec{u} = \vec{d}$$

So if the matrix could be inverted, we would have the solution. Now, if the numbering of the mesh points is done in a regular manner, it is easy to see that in the matrix \vec{A} , all the terms will be zero except those in a band whose width is of the order $N^{1/2}$ around the main diagonal.

Computer Solution. If we devise a computer program which takes advantage of these zeros, a 400 x 400 matrix may be stored in $400 \times 400^{1/2} = 8000$ cells instead of $(400)^2 = 160,000$. In such a case one need perform no calculations with the zeros off the diagonal band, enabling fast computation. Such a program, using Gaussian elimination and written by J. F. Holt of Space Technology Laboratories, solved the mesh indicated in Fig. 13 on an IBM 7090 in one minute.

In Fig. 14 we have indicated the values of Z'_0 and Z''_0 derived from the density data of Figs. 15 and 16. The surface profile comes from Iselin's surface densities. The large peak represents the warm core. First, a solution was attempted in which the solid line represented the boundary of the region. This solid line is the exact transcription of Iselin's surface data. The result of those calculations--that there is a sharp decrease in Δ at the extreme left edge--reflects the fact shown in Fig. 1 that isotherms 18°C through 12°C rise near the surface around Station 1229 but do not reach the surface until Station 1231. It is of interest that this side lobe of core water is not present in all of Iselin's section, where frequently the density lines come directly to

the surface. We might then conjecture that the lobe is an anomaly not reflecting the true dynamic structure of the stream. The dotted line, therefore, is drawn to indicate roughly what the boundaries would look like if the isotherms mentioned above came directly to the surface.

In support of this elimination of the core lobe, note that in the solution performed with the solid boundary, almost all the points between the dashed boundary and the solid boundary had, for a given r , larger values of Δ than the boundary value for that r . That is to say, the solution forced these lines of density to rise above the free surface-- which is, of course, physically impossible. The author feels that this is the correct solution to the equation and does not represent a computational error or a result of using finite differences.

In the solution (retaining the core), as mentioned, the lines of constant density (which largely parallel the lines of constant temperature) slope steeply to the right of Station 1231 due to the small boundary values of Δ near Station 1231. The true situation, seen in Fig. 1, is that the density lines are rather flat in this region. This certainly suggests that we should throw out the lobe and, shifting the solid line to the right as a first guess, perform the solution with the dashed lines as boundary. Values for parameters used in the solution were

$$h_0 = 2000 \text{ m}$$

$$2K = 1.79 \times 10^{-3}$$

$$f = 0.81 \times 10^{-4} \text{ sec}^{-1}$$

It is the solution performed within the dashed-line boundary which is written in schematically at a few of the total of 400 points in Fig. 14. This solution has been transformed to (x,z) co-ordinates in Fig. 17 which may be favorably compared with Fig. 1, the experimental data.

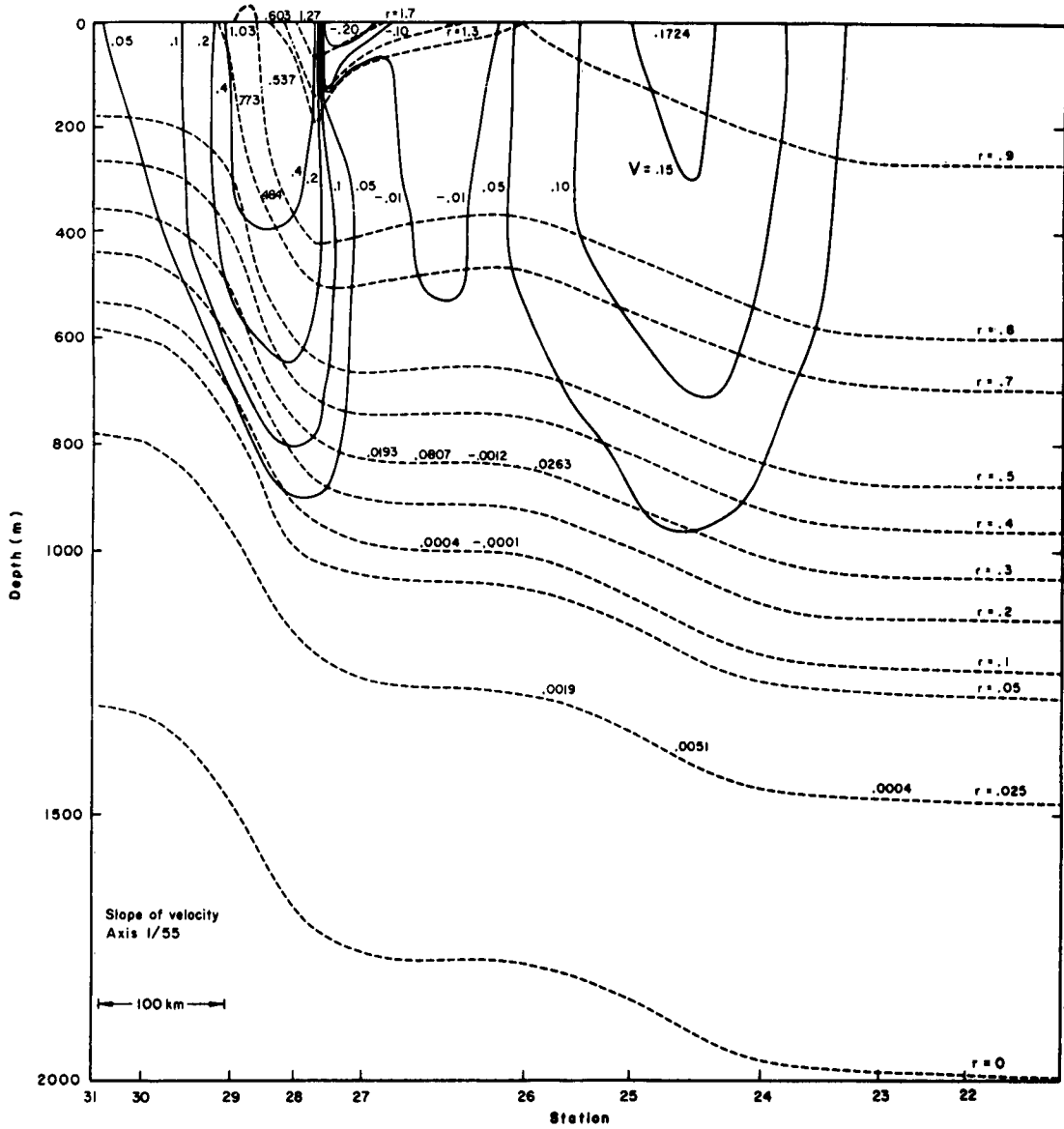


Fig. 17 -- Solution in (x, z) co-ordinates of the region bounded by the dotted line in Fig. 14 ($Z'_0(r)$ per Fig. 14; $\frac{\partial v}{\partial x} = 0$)

However, there are still a few delicate points in this solution. First, the inconsistency of the assumptions with the results in the core reflects our ignorance about the core's source region. The inconsistency could undoubtedly be corrected, simply if tediously, by the iterative procedure mentioned before. This would not change the qualitative solutions; it would in fact be only a formal manipulation. Secondly, we find that two points next to the bend in the dotted line rise just slightly out of the water. However, as shown in Fig. 17, the error is small and in context can only mean that we did not quite guess the true dynamic situation. With reference to this point, the whole pattern in Fig. 17 shows a shift somewhat to the left with reference to Fig. 1. This could in large measure be removed if the obtuse angle in the dashed line in Fig. 14 were moved right to form a right angle, showing the lines of constant density coming to the surface in a very small region. This would also alleviate the problem of their coming out of the water.

Since the density lines in Fig. 17 follow the observations so closely, there is little question that the velocities will agree with the observed ones, since we determine the velocities in this theory from the density field by directly applying the geostrophic equation.

Interestingly, the distance that the lines of constant density fall to their equilibrium height is accurately given, as is the slope of the axis of maximum current under the stream. We see that the core introduces a "plateau" in the deeper isotherms even though in the (x,z) co-ordinates the core looks rather insignificant.

One final discrepancy in the results should be mentioned. The isotherms do not rise to the proper height on the left. This is simply

due to a slightly erroneous boundary condition inserted into the computer. It could be easily remedied, but the agreement is sufficient as it stands for one to be assured of the theory.

III. CROMWELL CURRENT

Figure 18 shows a density cross section of the Cromwell Current.*
Figure 19 shows a salinity cross section at the same longitude in May
of 1958.

THEORY OF THE CROMWELL CURRENT

We will try to construct a theory of the Cromwell Current using ideas of potential vorticity. An earlier attempt in this direction was made by Fofonoff and Montgomery.⁽⁷⁾ They suggested that water flowed toward the equator in a layer of constant thickness, conserving potential vorticity; then at the equator it rose to the surface and spread to the north again only to sink and again move back toward the equator.

Now, Fig. 19 shows that there are widely varying salinities in a cross section. These data do not suggest that there is a cross-stream flow; they suggest jets unconnected laterally and moving east and west. This is verified in the report of King,⁽⁸⁾ which shows similar salinity cross sections at 140° , 120° , and 110° W. Further, if the northern and southern waters mixed at the equator, then the concept of potential vorticity of a water mass in this sinking and rising water would be even more nebulous than it is now; we might also expect to find uniform salinity throughout the section, since it would all have passed through the mixing process. On the other hand, if the water did not mix, and

*The author is indebted to John Knauss⁽⁶⁾ for this drawing and for all other density data on the Cromwell Current mentioned in his article. The data were obtained on the H. M. Smith at 140° W longitude, April 17 to 24, 1958.

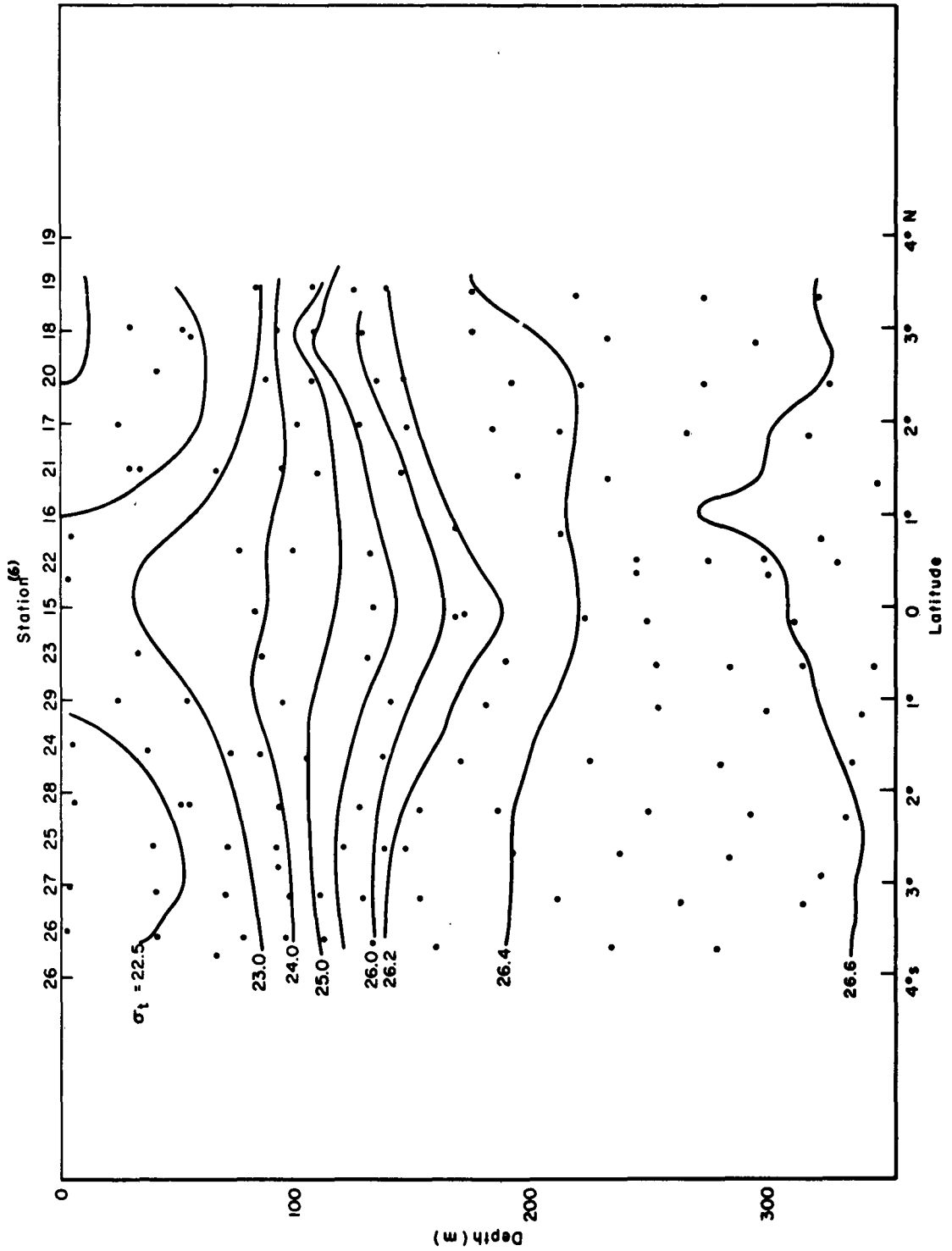


Fig. 18 -- Density cross section of the Cromwell Current

yet this circulation took place, then we might expect to see a variation in time of the salinity values at the equator as different parcels of water moved by. Such variations are absent in the data of repeated stations at the equator by Knauss. ^{(6)*}

It is true that the water at the equator is an approximate mean in salinity between the northern and southern water. Although this could show mixing, it indicates that the water in the stream comes from a slow-moving area in the west, where there is a similar regular variation of salinity across the equator.

It is of interest that this salinity cross section, as drawn by Knauss, ⁽⁶⁾ does not have the same extremely regular structure as the oxygen. Graphs showing phosphorus, in addition to oxygen and salinity, are also among those of King, ⁽⁸⁾ which are reproduced by Knauss. This may show that the oxygen and phosphorus distributions are governed not by vertical mixing but by the Cromwell Current's effect on some biological processes which do not affect salinity.

To gain a rough dynamical insight into whether or not it is reasonable, in view of the newer data, to say that water moves in the manner described by Fofonoff and Montgomery, we shall construct a simple model. We note first from Fig. 18 that in the region of swiftest current the isopycnics are practically linear between 0° and 3°N latitude. So we suppose that a layer's thickness, represented by h , is given by

$$h = (n - 1) h_0 (1 - y/y_0) + h_0 \quad (31)$$

* Despite these arguments, recent measurements by Knauss (personal communication) indicate such large (~ 20 m/sec) north-south velocities in the Cromwell Current, supporting the arguments of Fofonoff and Montgomery.

where h_0 is the thickness at $y = y_0$, and nh_0 is the thickness at $y = 0$. We see that n is the ratio of the thickness of a layer at the equator to its thickness at y_0 . We shall select $y_0 = 3^{\circ}N$ in this case. The equation for the conservation of potential vorticity then is

$$\frac{\beta y - \frac{\partial u}{\partial y}}{h} = \frac{\beta y_0}{h_0} \quad (32)$$

We note immediately that if we apply this equation to the south side also, replacing y_0 by $-y_0$, then at the equator where $y = 0$ there is a large unrealistic discontinuity in $\frac{\partial u}{\partial y}$.

Inserting Eq. (31) into Eq. (32) and integrating with the boundary condition $u = 0$ at $y = y_0$, we get

$$u = \frac{\beta n}{2} (y - y_0)^2 \quad (33)$$

The maximum value of n in the central core as picked off Fig. 18 is about 3. We then find that the maximum expected velocity is about 400 cm/sec. This is too large. Therefore, arguments against the north-south flow of water are the discontinuity of $\frac{\partial u}{\partial y}$ and, secondarily, the large velocity resulting from this assumption.

We might then suppose, in harmony with the salinity considerations, that the water came from a region where the water was moving slowly and the isotherms were horizontal across the equator. In this case, the water would come from a region of varying potential vorticity. For example, the water at the equator would have zero potential vorticity, in agreement with observation.

To describe this we would write in place of Eq. (32)

$$\frac{\beta y - \frac{\partial u}{\partial y}}{h} = \frac{\beta y}{h_0} \quad (34)$$

Carrying through the same manipulation as in Eqs. (31), (32), and (33), we find

$$u = \frac{\beta(n-1)}{6} \left\{ y_o^2 + 2y^3/y_o - 3y^2 \right\} \quad (35)$$

This time the maximum velocity is about 90 cm/sec, which is closer to observation, and there is no discontinuity at the equator. Furthermore, when $n < 1$, as actually occurs below 200 m, we get a countercurrent. The model breaks down near the surface, since the lines of constant density are no longer straight lines. However, we see that $n < 1$ (roughly) there also.

Now, it should be noted that if we write the equation of potential vorticity in the form

$$\frac{\beta y - \frac{\partial u}{\partial y}}{h} = \frac{\alpha \beta y}{h_o} \quad (36)$$

we cannot, for reasons of continuity, expect the equation to be correct with $\alpha = 1$ because the water must come in from the side as the stream moves from west to east, with its layers thickening and velocities increasing; α then represents the latitudinal extent of the source region. For example, if $\alpha = 2$, we will imagine that the water found at $2^\circ N$ began its rapid movement toward the equator at $4^\circ N$. We remember in this regard that the source region of the Gulf Stream was measured in thousands of kilometers, while the width of the stream itself was measured in hundreds of kilometers.

If we carry through the model above with an α , we find

$$\frac{u}{y_o^2 \beta} = \left[1/2 (\alpha n - 1) \left(1 - \left(\frac{y}{y_o} \right)^2 \right) - 1/3 \alpha (n - 1) \left(1 - \left(\frac{y}{y_o} \right)^3 \right) \right]$$

Here, if we put $\alpha = 1.25$, we find the maximum velocity to be 140 cm/sec. This small value of α suggests that the stream brings in water from near the equator over a long longitudinal distance.

ONE-LAYER MODEL

We now construct a one-layer Cromwell Current model analogous to Stommel's Gulf Stream model. We use Eq. (36) with the geostrophic equation

$$\beta y u = -g' \frac{\partial h}{\partial y} \quad (37)$$

and get

$$\frac{\partial^2 h}{\partial y^2} - \frac{1}{y} \frac{\partial h}{\partial y} - \frac{\alpha \beta^2 y^2}{g' h_0} h = - \frac{\beta^2 y^2}{g'} \quad (38)$$

Introducing as dimensionless variables

$$\hat{h} = \frac{h}{h_0}, \quad \hat{y} = y \gamma^{1/4}, \quad \gamma = \frac{\beta^2}{g' h_0}$$

we get

$$\hat{y} \frac{\partial^2 \hat{h}}{\partial \hat{y}^2} - \frac{\partial \hat{h}}{\partial \hat{y}} - \alpha \hat{y}^4 \hat{h} = - \hat{y}^4 \quad (39)$$

The solution to this is

$$\hat{h} = a e^{+\alpha^{1/2} \hat{y}^{2/3}} + b e^{-\alpha^{1/2} \hat{y}^{2/2}} + 1 \quad (40)$$

Discarding the growing exponential for finiteness at infinity, we get

$$\hat{h} = b e^{-\alpha^{1/2} \hat{y}^{2/2}} + 1 \quad (41)$$

Setting $\hat{h} = n$ at $\hat{y} = 0$, we find $b = n - 1$; therefore

$$h = h_0 (n - 1) e^{-\alpha^{1/2} \hat{y}^{2/2}} + h_0 \quad (42)$$

$$u = \alpha^{1/2} (n - 1) \sqrt{g' h_0} e^{-\alpha^{1/2} \hat{y}^{2/2}}$$

These results suggest substituting $\xi = \hat{y}^2/2$ in Eq. (39). This gives

$$\frac{\partial^2 \hat{h}}{\partial \xi^2} - \alpha \hat{h} = -1 \quad (43)$$

We see that we have recovered the sort of equation we solved for the Gulf Stream; thus we will plan to make this substitution in the continuous case also.

Continuous Case of the Cromwell Current

The equation corresponding to Eq. (15) is

$$\frac{\partial u}{\partial y} = -\frac{\beta y \alpha}{z'_0} \frac{\partial \Delta}{\partial r} - (\alpha - 1)\beta y \quad (44)$$

As we noted previously, Eq. (19) holds also in the y direction, so we have, also analogous to Eq. (21)*

$$\left(\frac{\partial p}{\partial y} \right)_z = -\rho f u = -2Kg\rho_b \int_{r_b}^r \frac{\partial \Delta}{\partial y} dr \quad (45)$$

So in this case

$$u = \frac{2Kg}{\beta y} \int_{r_b}^r \frac{\partial \Delta}{\partial y} dr \quad (46)$$

Despite the additional term in Eq. (44), the analysis follows as before. Differentiating the right-hand side of Eq. (45), first with respect to y and then with respect to r, and equating it to the right-hand side of Eq. (44), differentiated with respect to r, we get

*Robinson⁽⁹⁾ has justified the use of the geostrophic relation in the second momentum equation within 2 to 10 km of the equator.

$$\frac{2Kg}{\beta y} \frac{\partial^2 \Delta}{\partial y^2} - \frac{2Kg}{\beta y^2} \frac{\partial \Delta}{\partial y} = -\beta y \alpha \left\{ \frac{1}{z'_o} \frac{\partial^2 \Delta}{\partial r^2} - \frac{z''_o}{z'^2_o} \frac{\partial \Delta}{\partial r} \right\} \quad (47)$$

Making the substitutions

$$\hat{y} = y \left(\frac{\beta^2}{2Kgh_o} \right)^{-1/4} = \frac{y}{y_b}$$

$$\hat{\Delta} = \frac{\Delta}{h_o}$$

$$\hat{z}_o = \frac{z_o}{h_o}$$

we get, using primes for r differentiation

$$\frac{1}{y^2} \frac{\partial^2 \Delta}{\partial \hat{y}^2} - \frac{1}{y^3} \frac{\partial \Delta}{\partial \hat{y}} = -\alpha \left\{ \frac{1}{\hat{z}'_o} \frac{\partial^2 \hat{\Delta}}{\partial r^2} - \frac{\hat{z}''_o}{\hat{z}'^2_o} \frac{\partial \hat{\Delta}}{\partial r} \right\} \quad (48)$$

Under the substitution $\xi = \hat{y}^2/2$ this becomes

$$\frac{\partial^2 \hat{\Delta}}{\partial r^2} + \frac{\hat{z}'_o}{\alpha} \frac{\partial^2 \hat{\Delta}}{\partial \xi^2} - \frac{\hat{z}''_o}{\hat{z}'_o} \frac{\partial \hat{\Delta}}{\partial r} = 0 \quad (49)$$

The equation for the velocity becomes

$$u = \sqrt{2Kgh_o} \int_{r_b}^r \frac{\partial \hat{\Delta}}{\partial \xi} dr$$

And we see that we have precisely the same mathematical problem as for the Gulf Stream.

Cromwell Current Data

In the case of the Cromwell Current it will be necessary to specify the surface boundary condition, $\Delta = 0$ at infinity to the north, and $\Delta(r)$ at the equator. To specify $\Delta(r)$, two accurate density sections are needed--one at the equator and another around $4^\circ N$ or S. For the section

at the equator, five stations from the R. V. Horizon, April 7 to 11, 1958, were averaged, and the result is plotted in Fig. 20. For the station to the north from which Δ 's are to be measured, four H. M. Smith stations from 3° and 3.5° N and S latitudes were plotted on one graph, and a smooth line was drawn between them. This is seen in Fig. 21.

To obtain Δ as a function of ρ , a value of ρ was selected in Fig. 21 and also found in Fig. 20. The difference in depth was divided by 1000 m, thus giving $\hat{\Delta}(r)$. In Fig. 22, $\hat{\Delta}$ is plotted as a function of r at the equator.

In Fig. 23, we see a plot of the region in which we are to solve Eq. (49) in (r, θ) co-ordinates, together with the surface profile drawn from pertinent H. M. Smith stations. On the left side, the solid line shows $\hat{\Delta}(r)$; \hat{Z}'_0 and \hat{Z}''_0 are also seen as computed from the straight line drawn in Fig. 21. In the mesh which is to be solved, there are 285 boundary and interior points.

Before proceeding to the complete solution, it might be profitable to make a simple continuous model. For this purpose we model $\hat{\Delta}(r)$ at the equator by the cosine function shown by the dotted line at the left in Fig. 23. In this simple model we imagine a linear density gradient and also a surface boundary condition to be imposed by the solution.

It is easily seen that an appropriate solution satisfying the above conditions is

$$\Delta = \Delta_0 \cos 2\pi r e^{-2\pi \xi \alpha^{1/2}} \quad (50)$$

$$u = \sqrt{2Kgch_0} \hat{\Delta}_0 \sin(2\pi r) e^{-2\pi \xi \alpha^{1/2}}$$

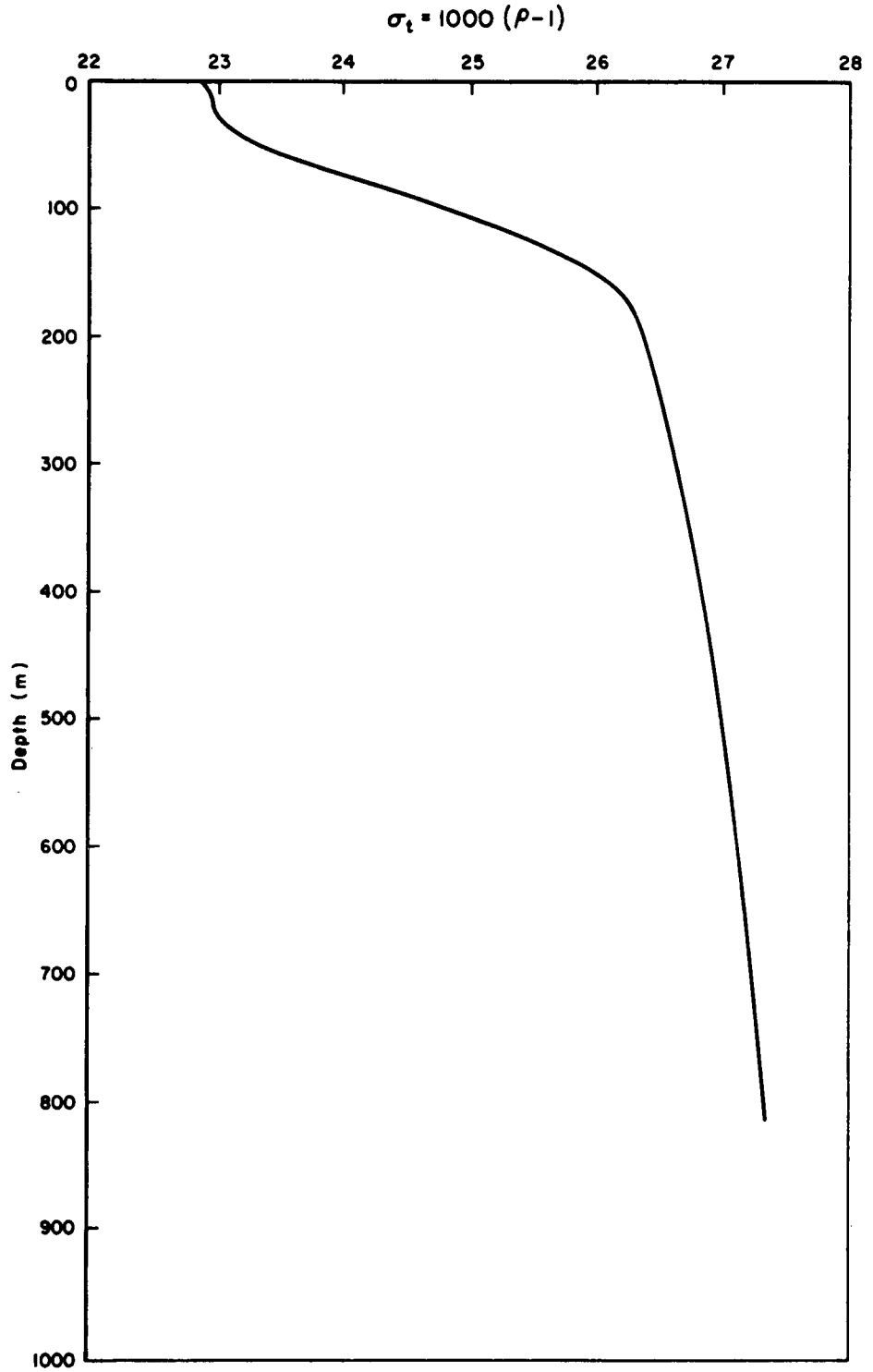


Fig. 20 -- Average of five stations 0°N Lat., 140°W Long.

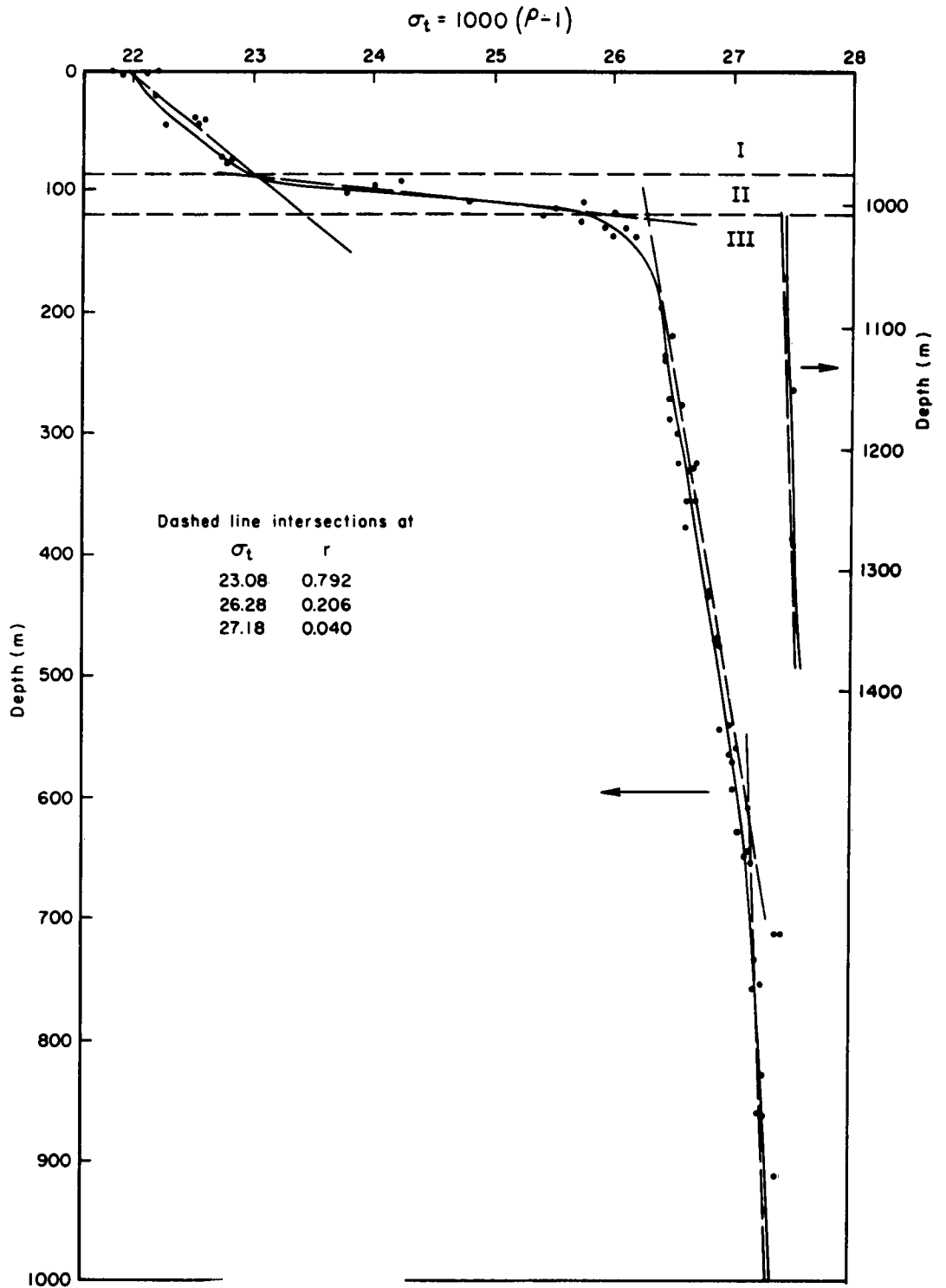


Fig. 21 -- Average of four stations at
3° and 3.5°N and S, 140°W

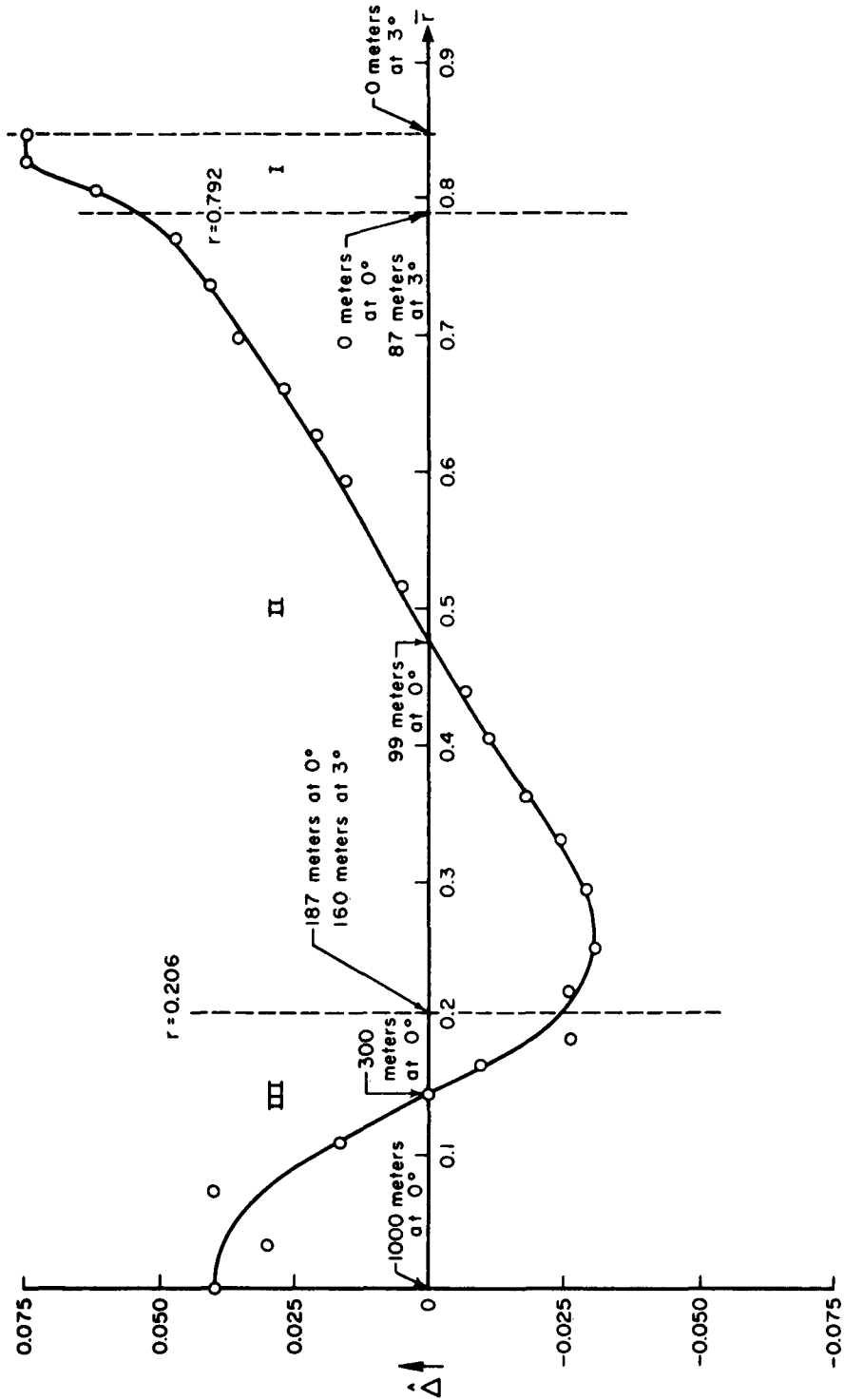


Fig. 22 -- $\hat{\Delta}$ at $0^\circ N$, $140^\circ W$ --based on Figs. 20 and 21

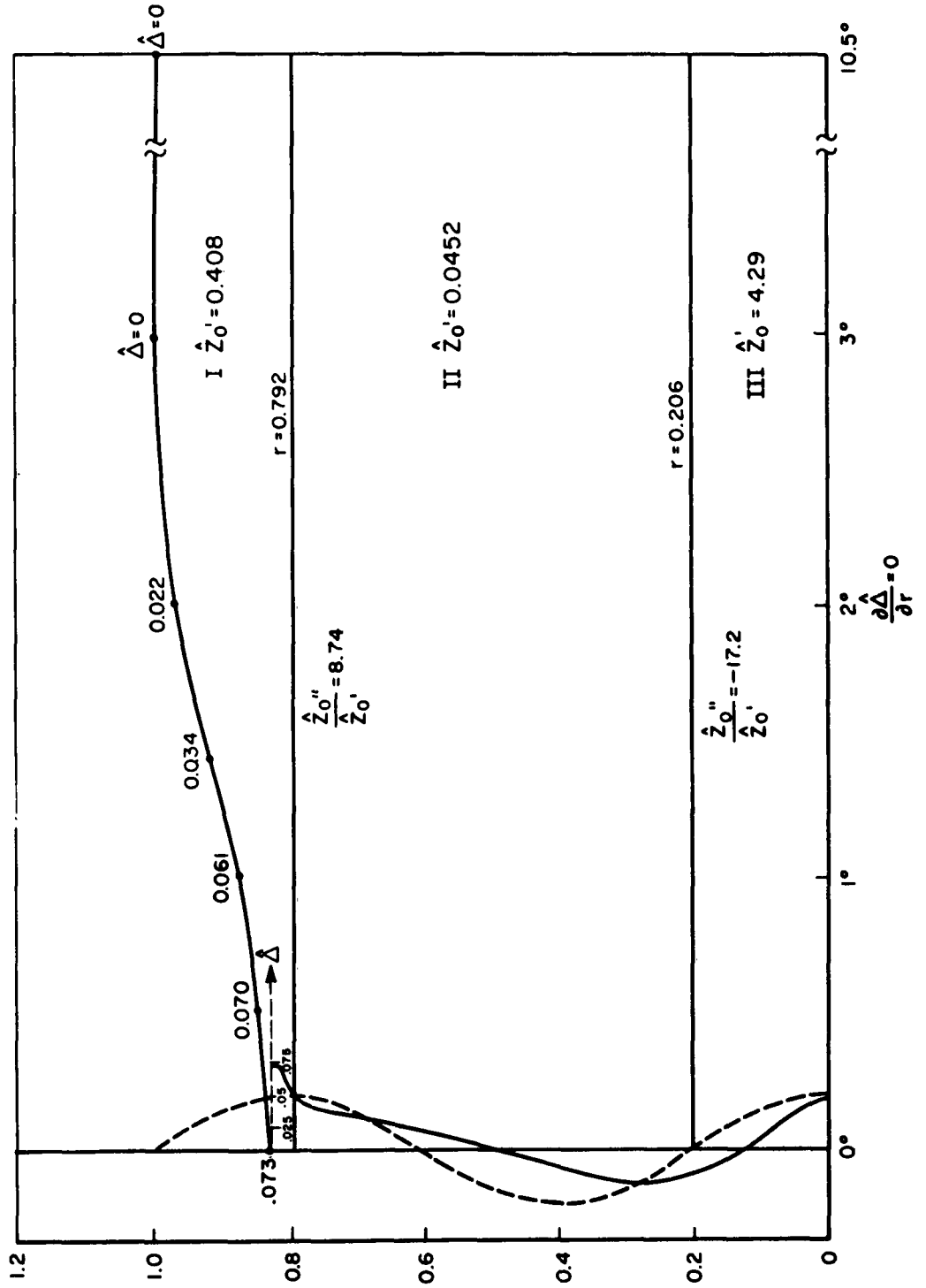


Fig. 23 -- Region for solution of Crowell Current in (r,θ) co-ordinates

We see that the characteristic fall-off distance for Δ , y_{ch} , is obtained by setting $2\pi\epsilon\alpha^{1/2} = 1$, or

$$y_{ch}^2 = \frac{y_b^2}{\pi\alpha^{1/2}}$$

where

$$y_b = \left(\frac{2Kgh_o}{\beta^2} \right)^{1/4}$$

To keep from straining the linear-density-gradient approximation more than we have already, suppose we take

$$\begin{aligned} h_o &= 700 \text{ m} \\ 2Kg &= 3.6 \times 10^{-2} \\ \beta &= 2.3 \times 10^{-13} \text{ m}^{-1} \text{ sec}^{-1} \end{aligned}$$

Then

$$\begin{aligned} y_o &= 456 \text{ km} \\ y_{ch} &= \frac{258}{\alpha^{1/4}} \text{ km} \end{aligned}$$

Now the observed value for y_{ch} is about 150 km. This suggests that α might be about 9. But this neglects an important fact which we can see in Fig. 23. For most values of r , Z'_o is about 1/20 instead of 1, which was implicit in the assumption of a linear-density gradient. The smaller value of Z'_o will make the constant-density lines fall off much more rapidly than before. We see that a linear-density approximation is extremely poor and cannot be trusted. Similar conclusions are obtained by evaluating the velocities due to this simple model. However, one point worth noting is that there is no westward surface current in this model. This is due to a mistreatment of the surface boundary condition in this simple model, which assumes that the surface has constant density.

Computer Solution

Now we continue with the complete solution of this model of the Cromwell Current. The problem is as sketched in Fig. 23. The actual co-ordinates in which Eq. (49) is solved numerically are (ξ, r) co-ordinates. This requires spacing which was much more variable in the ξ co-ordinate than that used in the x co-ordinate for the Gulf Stream if we hope to get values for the current both near and far away from the equator, using a reasonable number of mesh points. For example, 0.1° corresponds to $\xi = 2 \times 10^{-4}$, and 5° corresponds to $\xi = 5 \times 10^{-1}$. As a result of the highly variable spacing, the elements of the matrix for inversion varied by a factor of 10^6 . However, extra precision was used in the inversion, the results are smooth, and there is no reason to suspect errors. Perhaps it should be noted here that a priori there is no good reason to expect excellent results from this theory, even with α as an adjustable parameter because, for example, there is no reason to suppose that all the water at a given latitude in the stream originated at the same latitude. Two facts save us: α , in agreement with the discussion after Eq. (36), is close to 1; and the solution is relatively insensitive to the value of α . In fact, as can be seen from the simple model just presented, the decay distance of Δ is roughly proportional to $\alpha^{1/4}$, and the velocity to $\alpha^{1/2}$.

The region in which the equation was solved extended to $\xi = 2$, or about 10.15° . In the numerical solution, all the values of Δ had declined by factors of at least 20 by 5° , so that the solution effectively did extend to infinity away from the equator.

In Fig. 24 the complete solution is drawn in (Z, θ) co-ordinates. By comparing with Figs. 25 and 26 from Knauss,⁽⁶⁾ we see that the

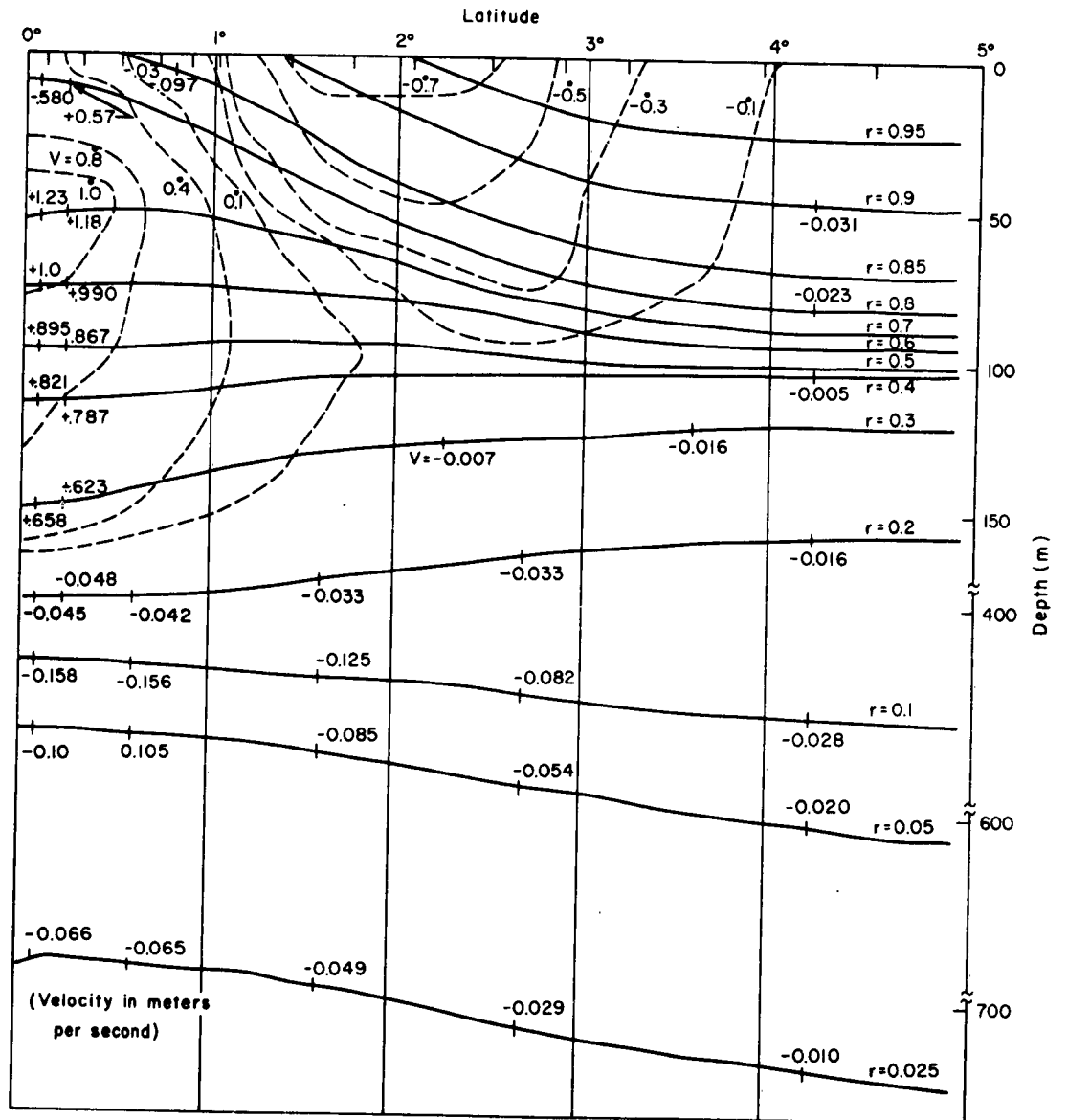


Fig. 24 -- Numerical solution of Fig. 23 expressed in (z,θ) co-ordinates

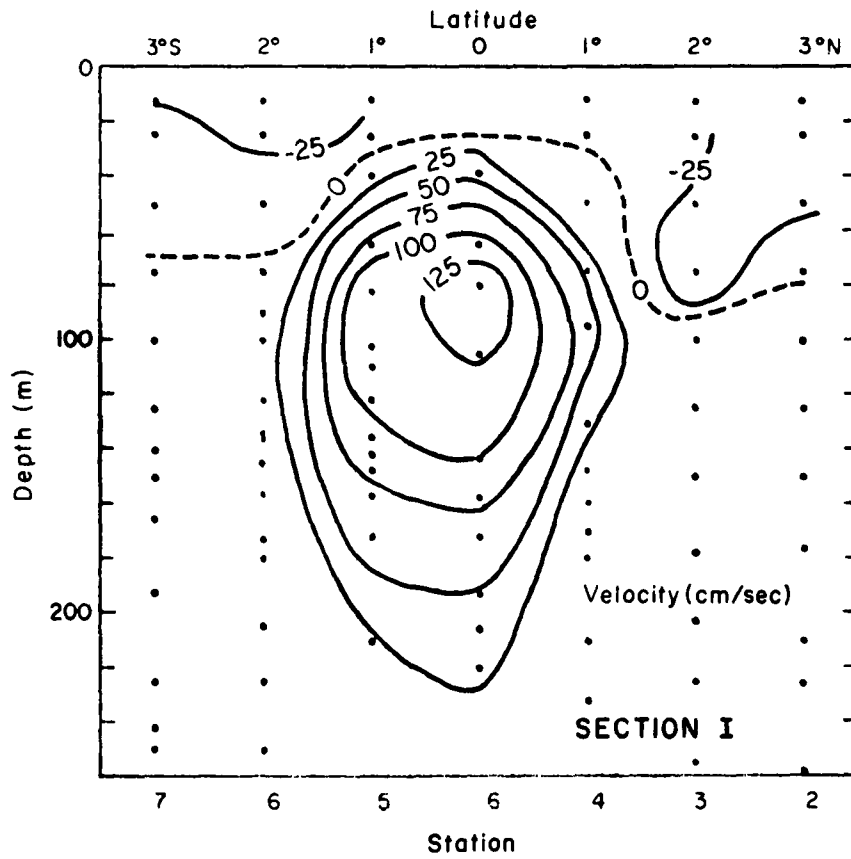


Fig. 25 -- Observed velocity
cross section at 140°W⁽⁶⁾

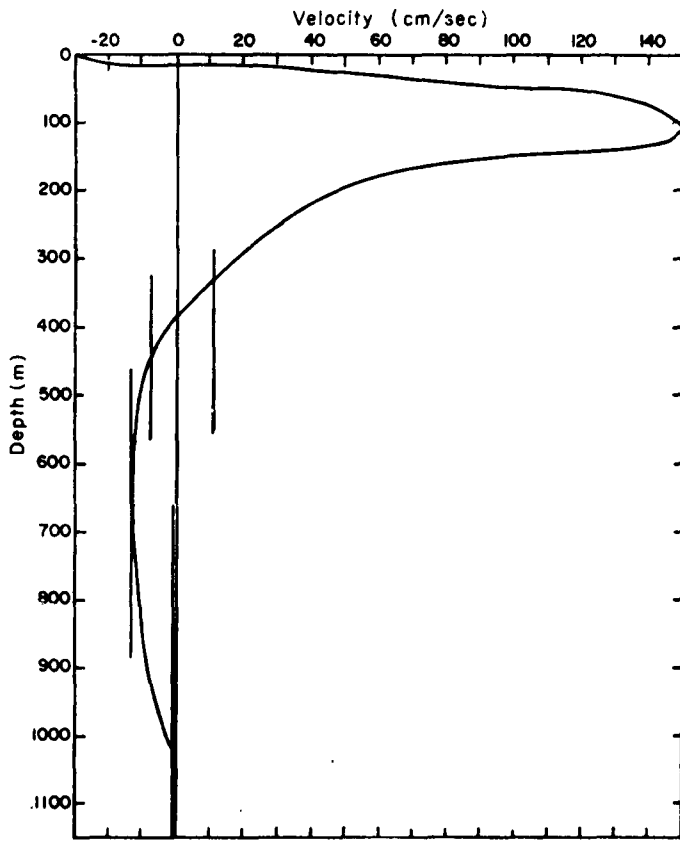


Fig. 26 -- A composite east-west current profile at the equator at 140°W⁽⁶⁾

undercurrent is displaced somewhat upwards from observation, that the velocity is too slow, and that the decay distance is slightly too large. These last two effects can undoubtedly be corrected by introducing an α of about 1.4. In agreement with our first simple dynamical model, this shows that the source of the water in the Cromwell Current is not very far from the equator, and thus that the current must grow slowly as it moves across the Pacific--not all at once in a few degrees of longitude.

The upward displacement of the undercurrent may be an effect of vertical friction, as discussed in Appendix B. Or, since the density lines so closely parallel the true ones, it might show a failure of the geostrophic equation, $\beta_y = \frac{1}{\rho} \frac{\partial \rho}{\partial y}$. However, it is barely conceivable that it could also be due to a combination of small errors in the calculation of $\hat{\Delta}$ at the equator (Fig. 22), poor values of r on the surface between 0° and 0.5° , and finally a true level of transition between the undercurrent and the deep current at 300 m instead of 400 m as drawn by Knauss. That this is possible we see from the error limits on the deep velocity as drawn in Fig. 26.

Perhaps it should be emphasized at this point that there is no boundary condition in this problem forcing $\hat{\Delta}$ to go to 0 anywhere short of 10°N , and so the fact that $\hat{\Delta}$ goes to 0 more or less as observed is a nonimposed result of the theory.

The theory gives larger values than observed for a surface current between 1.5° and 2.5° . This is a direct reflection of the large surface density gradient and is extremely sensitive to the surface density data. Nevertheless, there is not much room for manipulation of the data

available at the present to escape this result. Therefore, these large values are a real result of the theory. However, since the calculated density lines follow so closely the observed ones, it seems difficult to explain the discrepancy except by a failure of the geostrophic equation. Perhaps they reflect an Ekman layer. These large values of the velocity would only be increased by increasing α .

One explanation might be that, as we see in Fig. 18, some of the density lines rise around 3° as they move away from the equator. This behavior has been excluded by the theory and yet might slow down the surface current. The effect may also show the influence of the wind near the surface.

The sporadic behavior of the surface current near the equator possibly results from a lack of surface-density data, to which the surface current is extremely sensitive. A linear extrapolation between 0.5° and 0° was used, and it gave these strange results. Perhaps better surface-density data would give the proper currents.

In agreement with observation, some density lines around 100 m reach a maximum elevation around 1° and then decline toward the equator.

The density lines below 400 m are about 5 m from their asymptotic elevation at $x = \infty$ when they run off Fig. 24.

IV. CONCLUDING REMARKS

Excellent agreement with observation has been obtained using potential-vorticity theorems with no arbitrary parameters for both the Gulf Stream and the Cromwell Current. These results indicate small values for the eddy-viscosity coefficients. It is predicted that the Cromwell Current grows slowly as it crosses the Pacific and does not appear full-blown in a few degrees of longitude, nor does the water in it move toward and away from the equator in the manner suggested by Fofonoff and Montgomery. This should have important implications for a causal theory. The problems of the detailed dynamics of these streams have therefore been shown to be equivalent to predicting the density structures on the surface and in one or two sections, and to knowing some characteristics of the source region. There is some need for more detailed data at the surface of the Cromwell Current to improve the calculations.

Even though the theory is noncausal, it could provide a framework for other studies. For example, our simple continuous model of the Gulf Stream might be useful for an analytical study of internal waves on the Gulf Stream, or in a stability analysis.

Appendix A

THE CONTINUOUS-MODEL CORE

Stommel's model (pp. 4-14) can be extended to a fully three-dimensional model by at least two equivalent analytical techniques. One is to satisfy the Bernoulli integral on the stream-line which runs along the coast. Another is to insist that the flux moving into the coast below a given latitude equal the flux moving north across it in the Gulf Stream. Either requirement determines the depth of the upper layer along the coast and thus a complete solution. When the layer thickness goes to zero we have the cross-section of Eq. (4). In models of more than one layer, satisfying the Bernoulli integral will give the relationship at a given latitude between the boundary thicknesses of the several layers. In this Memorandum we have assumed these values to be known from observation. It would be a coincidence if we picked values which gave, for any latitude, a proper cross section for a solution which satisfied the Bernoulli integral. In fact, it can be shown analytically that the models on pages 19 and 33 do not satisfy the Bernoulli integral at any latitude. However, they still illustrate the types and quality of results obtainable by the use of constant potential vorticity and are valuable on that account. Also, the continuous calculation in Fig. 17 and Fig. 27 so precisely uses observed boundary conditions that one may hope that detailed calculation would show the Bernoulli integral to be satisfied. Thus, in the main, this work must be regarded as a preliminary exploration of the types of results perhaps obtainable in more rigorous fashion by dynamical boundary conditions. The good qualitative agreement obtained gives encouragement to further efforts to construct such a theory.

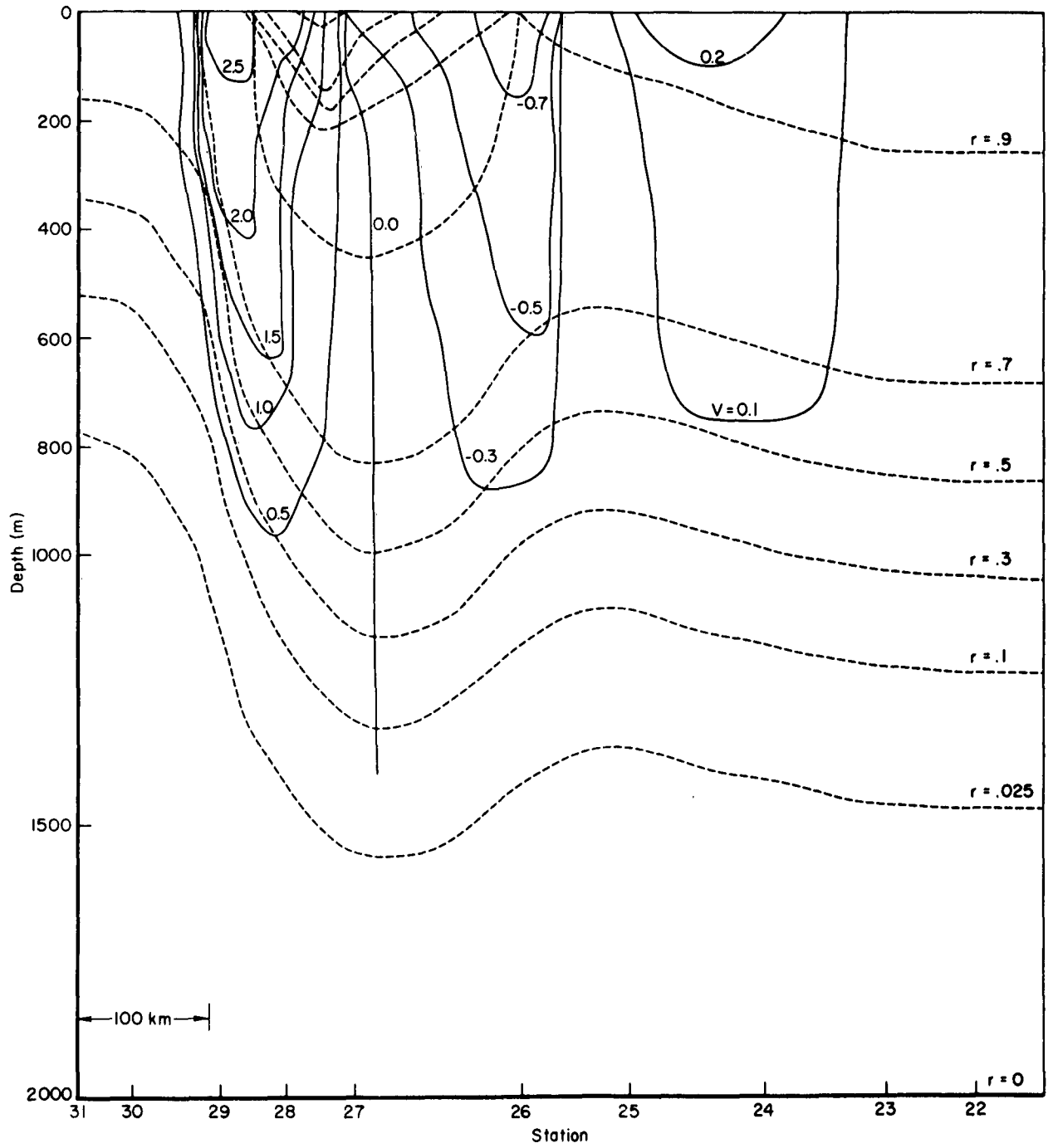


Fig. 27 -- Solution in (x,r) co-ordinates of the region bounded by the dotted line in Fig. 14 (5 times $Z'_0(r)$ per Fig. 14; $\frac{\partial v}{\partial x} \angle 0$)

The treatment of the core in the continuous model on pages 37-39 is unnecessarily forced and arbitrary. It has been replaced by another treatment, and the continuous calculation repeated. The result is shown in Fig. 27.

To discuss this new technique, let us set the vertical scale by assuming $Z_0(1) = 0$. (See p. 27)

Then

$$Z_0(r) = \int_1^r Z'_0(r) dr$$

From the definition of Δ before Eq. (15), we see that at the surface the boundary condition is $\Delta = -Z_0(r)$. (Remember that $z(r) = 0$ at the upper boundary.) Thus we may determine the boundary condition on the water in the core from the observed values of $Z'_0(r)$ in the core.

When the values of $Z'_0(r)$ shown in Fig. 16 were used in calculation, the resulting solution was physically impossible. The solution was physically reasonable only for value of $Z'_0(r)$ in the core from 4 to 6 times that shown in Fig. 16. A factor of 5 was used for the calculations leading to Fig. 27. This is consistent with the facts that the water in the core is advected from lower latitudes and that there is a large horizontal velocity shear in the core, of such a sign that the observed $\frac{\partial z}{\partial r}$ is smaller than $\frac{\partial Z_0}{\partial r}$. Since we cannot precisely identify the source of the core water there is no reliable way of evaluating this multiplicative constant within the present theory except to say that it must be greater than unity for $\frac{\partial v}{\partial x} < 0$. (See Eq. (1)). The fact that the present calculation gives such a factor is encouraging.

Appendix B

DERIVATION OF POTENTIAL-VORTICITY EQUATION

This appendix gives a derivation of the potential-vorticity equation after the manner of Eliasson and Kleinschmidt⁽¹⁰⁾ and also gives estimates of the error due to friction.

DERIVATION OF POTENTIAL-VORTICITY EQUATION

The equation of motion in an absolute inertial system is

$$\frac{d\mathbf{v}}{dt} = -\nabla\phi - \alpha\nabla p + \mathbf{K} \quad (51)$$

where p is the pressure, α the reciprocal of the density, $\nabla\phi$ the forces derivable from a potential, and \mathbf{K} all the other forces, such as friction.

Equation (51) may be written

$$\frac{\partial\mathbf{v}}{\partial t} + (\nabla \times \mathbf{v}) \times \mathbf{v} + \nabla(1/2 v^2) = -\nabla\phi - \alpha\nabla p + \mathbf{K} \quad (52)$$

Taking the curl of Eq. (52) we get

$$\frac{\partial\mathbf{q}}{\partial t} + \nabla \times (\mathbf{q} \times \mathbf{v}) = (\nabla \times \mathbf{K}) + \mathbf{S} \quad (53)$$

where $\mathbf{q} = \nabla \times \mathbf{v}$ and $\mathbf{S} = \nabla\alpha \times \nabla p$. Equation (53) may be expanded, and by using $\nabla \cdot (\nabla \times \mathbf{v})$ and recombining we get

$$\frac{d\mathbf{q}}{dt} + \mathbf{q}(\nabla \cdot \mathbf{v}) - (\mathbf{q} \times \nabla) \cdot \mathbf{v} = (\nabla \times \mathbf{K}) + \mathbf{S} \quad (54)$$

If we define

$$\chi = \mathbf{q} \cdot \alpha \nabla \psi \quad (55)$$

then

$$\frac{d\chi}{dt} = \frac{d\mathbf{q}}{dt} \cdot \alpha \nabla \psi + \mathbf{q} \cdot \left(\frac{d\alpha}{dt} \nabla \psi + \alpha \frac{d(\nabla \psi)}{dt} \right) \quad (56)$$

We have the identity

$$\frac{d(\nabla\psi)}{dt} = \nabla\left(\frac{d\psi}{dt}\right) - \nabla v \cdot \nabla\psi \quad (57)$$

Note that the last term on the right, like the others, is a vector.

Expanding $\frac{dq}{dt}$ by Eq. (54) and substituting Eq. (57), Eq. (56) becomes

$$\frac{dX}{dt} = \alpha \nabla\psi \cdot \frac{dq}{dt} + q \cdot \left\{ \frac{d\alpha}{dt} \nabla\psi + \alpha \left(\nabla\left(\frac{d\psi}{dt}\right) - \nabla v \cdot \nabla\psi \right) \right\} \quad (58)$$

Since $\frac{d\alpha}{dt} = \alpha(\nabla \cdot v)$ is the equation of continuity,

$$\frac{dX}{dt} = \alpha \nabla\psi \cdot \left\{ (S + \nabla \times K) + (q \cdot \nabla)v \right\} + q \cdot \left\{ \alpha \left(\nabla\left(\frac{d\psi}{dt}\right) - \nabla v \cdot \nabla\psi \right) \right\} \quad (59)$$

It may be easily verified that

$$\nabla\psi \cdot (q \cdot \nabla)v = q \cdot (\nabla v \cdot \nabla\psi) \quad (60)$$

If ψ is conserved, then $\frac{d\psi}{dt} = 0$; and if $\psi = g(\rho)$, then

$$\nabla\psi \cdot S = 0$$

Since

$$S = \nabla\left(\frac{1}{\rho}\right) \times \nabla p$$

then

$$\frac{dX}{dt} = \alpha \nabla\psi \cdot (\nabla \times K) \quad (61)$$

And if

$$\psi = \rho$$

then

$$\frac{d}{dt} (\text{curl } v \cdot \frac{1}{\rho} \nabla\rho) = \frac{1}{\rho} \nabla\rho \cdot (\nabla \times K) \quad (62)$$

And if

$$K = 0$$

then

$$\frac{d}{dt} (\text{curl } v \cdot \frac{1}{\rho} \nabla\rho) = 0 \quad (63)$$

Now in fact we assert $\psi = \rho$ and $\underline{\kappa} = 0$. So we may define a co-ordinate system whose "vertical" co-ordinate is this density. Define the rate of change of this co-ordinate for a given particle of water as its "vertical" velocity. This is clearly zero if the density is conserved. Now define, in the layers of constant density, vectors perpendicular to the gradient of the density. This constructs an orthogonal co-ordinate system. In this co-ordinate system, $\nabla\rho$ has only one nonzero component, which is in the same direction as the vertical component of $\text{curl } \underline{v}$. Since we have an orthogonal system, the dot product in Eq. (62) gives only one term, the product of the "vertical" component of the curl and the gradient of the density. Perhaps we might emphasize at this point that the vertical discussed above is not generally in the same direction as the gradient of the geopotential, or the vertical defined by the radial component of the coriolis force. Nevertheless, this is a completely general theorem. The only approximations are that friction may be neglected, that density surfaces may be defined, and that density is conserved along streamlines.

Returning to Eq. (62), $\text{curl } \underline{v}$ is the absolute vorticity with respect to an inertial system. Let us call the velocity with reference to the Earth \underline{u}_r , and that with respect to the inertial system \underline{u}_a , for the purpose of this brief discussion. Then

$$\underline{u}_a = (\underline{u}_r + \underline{\omega} \times \underline{r}) \quad (64)$$

where $\underline{\omega}$ is the Earth's angular velocity and \underline{r} is the Earth's radius.

So

$$(\nabla \times \underline{u}_a) = (\nabla \times \underline{u}_r) + \nabla \times (\underline{\omega} \times \underline{r}) \quad (65)$$

Inserting this into Eq. (62) we see that $\nabla\rho$ picks out the component of

the coriolis force parallel to itself. The value of this component is of course very close to $2\omega \sin \theta$.

If we call this component f and perform the dot product, then Eq. (63) becomes

$$\frac{d}{dt} \left\{ (\text{curl}_H \underline{v} + f) \cdot \left(\frac{1}{\rho} \nabla \rho \right) \right\} = 0 \quad (66)$$

where $\text{curl}_H \underline{v}$ is the curl of the horizontal velocity.

In this Memorandum we apply the theorem to specific cases as follows: In the source region we observe the value of $\frac{1}{\rho} \nabla \rho \cdot \left\{ \text{curl} \underline{u}_r + \nabla \times (\underline{\omega} \times \underline{r}) \right\}$.

Now in any of the co-ordinate systems mentioned above, this dot product has one term--the product of the "vertical" components--which is much larger than the others. So no matter which of these systems we pick, we get essentially the same number for the observed potential vorticity if we take only the product of the vertical components.

Now let us imagine that we follow the water flowing and we apply the theorem in the correct co-ordinate system to guarantee that when we look at $\nabla \rho \cdot (\text{curl} \underline{u}_r + \nabla \times \underline{\omega} \times \underline{r})$ again at some new point along the streamline we will find the same value. Then at the new point we shall again write approximate equations.

All the actual mathematics in the body of this Memorandum deals with these approximate equations; there is no need to explicitly treat the highly distorted, time-varying-density co-ordinate system. Nonetheless, it should be kept in mind that it is the conservation theorem holding in this co-ordinate system which enables us to write the approximate equations. (There may be cases in geophysics, and especially in model experiments, where the difference in verticals is not negligible.)

Note especially that using the theorem in this manner makes it independent of the hydrostatic assumption.

For an example of application we treat the Gulf Stream system. In its source region we observe that the distance between two isotherms, divided by the local coriolis parameter, is about a constant. In evaluating this constant, it makes no practical difference which of the three possible verticals we use; so we write simply $f/(\partial z/\partial \rho) = \text{constant}$, along lines of constant density. Now we imagine that the correct theorem "carries" the water to some cross section of the Gulf Stream. And so we write, along a line of constant density,

$$\frac{f + \frac{\partial v}{\partial x} - \frac{\partial u}{\partial y}}{\frac{\partial z}{\partial \rho}} = \text{constant or } \frac{f + \frac{\partial v}{\partial x} - \frac{\partial u}{\partial y}}{\frac{\partial z}{\partial \rho}} = g(\rho) \quad (67)$$

In the first pages of this Memorandum, potential vorticity is conserved in layers up to 800 m thick. Note that if we integrate Eq. (67) between two densities and consider the velocities to be constant in the range of integration, we get

$$\frac{f + \frac{\partial v}{\partial x} - \frac{\partial u}{\partial y}}{D} = \text{constant} \quad (68)$$

where D is the thickness of the layer.

Errors

The equation for conservation of potential vorticity, including friction, is

$$\frac{d}{dt} \left\{ \frac{1}{\rho} \underline{\nabla} \rho \cdot [\text{curl } \underline{v} + \nabla \times (\omega \times \underline{r})] \right\} \equiv \frac{d(\underline{\eta} \cdot \frac{1}{\rho} \underline{\nabla} \rho)}{dt} = \frac{1}{\rho} \underline{\nabla} \rho \cdot (\underline{\nabla} \times \underline{K}) \quad (69)$$

where $\underline{\eta} = [\text{curl } \underline{v} + \nabla \times (\omega \times \underline{r})]$

Using Eq. (69) we may now try to estimate the possible effects of friction on the foregoing theory. We estimate when the cumulative effect of

$(7 \times K)$, acting over the path of the water between the source and the point of observation, would be large enough to invalidate the theory. As a first approximation we might multiply $\dot{\eta}$ by the time necessary for the water to travel this path.

GULF STREAM

Let us consider vertical friction in the Gulf Stream. We have

$$\frac{\partial \eta}{\partial t} = \dot{\eta} \sim A_v \frac{\partial^3 v}{\partial x \partial z^2} \quad (70)$$

Therefore, we have, if the time necessary for travel from the Caribbean is L/v

$$\frac{\Delta \eta}{\eta} \sim \frac{\dot{\eta} \frac{L}{v}}{\frac{v}{\lambda}} \sim \frac{A_v L}{D_o^2 v} \sim A_v \times 10^{-2} \quad (71)$$

where

L = length of path = 2000 km

D_o = depth = 500 m

v = velocity = 10 cm/sec

λ = radius of deformation = 50 km

From this we see that, for the values of A_v currently seen in the literature (e.g., 5 or 10 cm^2/sec), the friction effect is small.

For the horizontal eddy viscosity

$$\dot{\eta} \sim A_H \frac{\partial^3 v}{\partial x^3} \quad (72)$$

This implies

$$\frac{\Delta \eta}{\eta} \sim \frac{A_H L}{\lambda^2 v} \sim A_H \times 10^{-6} \quad (73)$$

So we see that large values of the horizontal eddy viscosity would invalidate the theory, and we must have $A_h < 10^5 \text{ cm}^2/\text{sec}$ at least.

CROMWELL CURRENT ERRORS

Typical parameters for the Cromwell Current are

$$\begin{aligned} D &= 200 \text{ m} \\ L &= 10^4 \text{ km} \\ u &= 30 \text{ cm/sec} \\ \lambda &= 100 \text{ km} \end{aligned} \tag{74}$$

Then for the vertical eddy viscosity

$$\frac{\Delta\eta}{\eta} \sim \frac{A_v L}{D_o^2 u} \sim 10^{-1} A_v \tag{75}$$

So we see that a vertical coefficient of 5 or $10 \text{ cm}^2/\text{sec}$ might be serious, especially in the more slowly moving portions.

For the horizontal eddy viscosities we obtain much the same conclusion as for the Gulf Stream (i.e., $A_h < 10^6$), since

$$\frac{\Delta\eta}{\eta} \sim \frac{A_h L}{\lambda^2 u} \sim 3 \times 10^{-7} A_h \tag{76}$$

Of course it should be emphasized that these order-of-magnitude estimates do not conclusively show that any effect is unimportant or important because, for example, the expression for friction is quite hypothetical, and any given effect might be highly damped, or indeed be nonlinearly coupled and therefore produce a large effect.

REFERENCES

1. Stommel, H., The Gulf Stream: A Physical and Dynamical Description, University of California Press, Berkeley, 1958, p. 202.
2. Iselin, C. O'D, "A Study of the Circulation of the Western North Atlantic," Pap. Phys. Ocean. and Meteor., Vol. 4, No. 4, 1936, p. 101.
3. Neumann, G., "Zum Problem der Dynamischen Bezugflasche, Insbesondere in Golfstromgebiet," Deut. Hydrograph. Z., Vol. 6, 1956, pp. 66-78.
4. Worthington, L. V., "Three Detailed Cross-Sections of the Gulf Stream," Tellus, Vol. 6, 1954, pp. 116-123.
5. Rossby, C. G., "On the Mutual Adjustment of Pressure and Velocity. Distribution in Certain Simple Current Systems," J. Mar. Res., Vol. II, No. 1, 1938, pp. 239-263.
6. Knauss, J. A., "Measurements of the Cromwell Current," Deep-Sea Res., No. 6, 1960, pp. 265-286.
7. Fofonoff, N. P. and R. B. Montgomery, "The Equatorial Undercurrent in Light of the Vorticity Equation," Tellus, Vol. 7, 1955, pp. 518-521.
8. King, J. E., T. S. Austin, and M. S. Doty, "Preliminary Report on Expedition Eastropic," U.S. Fish Wildlife Service, Spec. Sci. Rept-Fish, No. 201, 1957, p. 155.
9. Robinson, A. R., "The General Thermal Circulation in the Equatorial Region," Deep Sea Res., Vol. 6, 1960, pp. 311-317.
10. Ellison, A. and E. Kleinschmidt, Handbuch der Physik, Vol. XLVII, 1957, pp. 1-154.